bioRxiv preprint doi: https://doi.org/10.1101/2021.11.16.468795; this version posted November 16, 2021. The copyright holder for this preprint (which was not certified by peer review) is the author/funder, who has granted bioRxiv a license to display the preprint in perpetuity. It is made available under aCC-BY-NC 4.0 International license.

Stimulation of immunity-linked genes by membrane disruption is linked to Golgi function and the ARF-1 GTPase

Christofer M. Welsh[1], Lorissa J. Smulan[2], Matthew J. Fanelli[1], Dominique S. Lui[1], and Amy K. Walker[1]

[1]Program in Molecular Medicine, UMASS Medical School, Worcester, MA

[2]Department of Medicine, UMASS Medical School, Worcester, MA

Contact: amy.walker@umassmed.edu

bioRxiv preprint doi: https://doi.org/10.1101/2021.11.16.468795; this version posted November 16, 2021. The copyright holder for this preprint (which was not certified by peer review) is the author/funder, who has granted bioRxiv a license to display the preprint in perpetuity. It is made available under aCC-BY-NC 4.0 International license.

Summary

Immune-linked genes (ILGs) are activated in response to pathogens but can also be activated by lipid imbalance. Why pathogen attack and metabolic changes both impact ILG activation is unclear. Organelles in the secretory pathway have distinct protein and lipid components and genetically separable stress programs. These stress pathways activate restorative transcriptional programs when lipid ratios become unbalanced or during dysregulated protein folding and trafficking. We find that ILGs are specifically activated when membrane phosphatidylcholine ratios change in the secretory pathway. Consistent with this result, disruption of Golgi function after RNAi targeting the ADP-ribosylation factor ARF-1 also activates ILG expression. Since increased protein secretion is altered by metabolic changes and pathogen responses, our data argue that ILG upregulation is a conserved, coordinated response to changes in trafficking resulting from intrinsic cues (lipid changes) or extrinsic stimulation (during the immune response). These findings uncover important and previously unexplored links between metabolism and the stress response.

bioRxiv preprint doi: https://doi.org/10.1101/2021.11.16.468795; this version posted November 16, 2021. The copyright holder for this preprint (which was not certified by peer review) is the author/funder, who has granted bioRxiv a license to display the preprint in perpetuity. It is made available under aCC-BY-NC 4.0 International license.

Introduction

Cellular stress responses both react to extrinsic insults by upregulating genes that defend the cell. Stress responses also restore organelle function in response to intrinsic changes. Several of these intrinsic stress response pathways are also linked to metabolic processes. For example, overnutrition can lead to metabolic changes that induce cellular stress through an increase in reactive oxygen species (Wellen and Thompson, 2010). Several signaling pathways play a dual role, functioning as coordinators of nutrient responses as well as stress responses. For example, the nutritional sensor mTORC1 can influence stress-responsive transcription (Aramburu et al., 2014). In addition, insulin signaling pathways are strongly linked to stress. For example, mutations in *daf-2*, the *Caenorhabditis elegans* insulin receptor/insulin-like growth factor ortholog, produce highly stress-resistant animals (Son et al., 2019). Finally, changes in ER lipids have a profound effect on stress pathways (Gianfrancesco et al., 2018; Halbleib et al., 2017; Koh et al., 2018). Specialized ER sensors detect both the accumulation of unfolded proteins and overload of the secretory pathway. These sensors then initiate gene expression programs that reduce protein load or increase lipid production (reviewed in: Hotamisligil and Davis, 2016; Radanović et al., 2018).

While stress responses and metabolism are clearly intertwined, the biological advantages of linking these processes are less clear. For example, in a previous study, we found that RNAi-mediated knockdown of two different lipid synthesis modulators, *sams-1* and *sbp-1*, caused upregulation of pathogen-response genes in *C. elegans* (Ding et al., 2015). One of these lipid modulators, *sams-1/MAT1A,* encodes an S-

bioRxiv preprint doi: https://doi.org/10.1101/2021.11.16.468795; this version posted November 16, 2021. The copyright holder for this preprint (which was not certified by peer review) is the author/funder, who has granted bioRxiv a license to display the preprint in perpetuity. It is made available under aCC-BY-NC 4.0 International license.

adenosylmethionine synthase important for phosphatidylcholine (PC) production (Walker et al., 2011). The Troemel lab also identified *sams-1* as a regulator of the infection response gene *irg-1* in an RNAi screen (Dunbar et al., 2012). The other lipid modulator identified in our previous screen, *sbp-1/SREBPF1,* codes for a master transcriptional regulator of lipid synthesis genes (Horton et al., 2002). Reduction of *sbp-1/SREBPF1* causes a decrease in total lipid stores (McKay et al., 2003). Notably, mammalian SREBPF1 knockdown also results in the enrichment of immunity-linked gene expression in human cells (Wu and Näär, 2019). Recent studies from other labs have found that ILGs are upregulated after mutation or RNAi of genes affecting PC synthesis. ILG activation was seen upon disruption of *pmt-2* (Ho et al., 2020) or *lpin-1* in the presence of excessive glucose (Jung et al., 2020). These immune-linked genes were also upregulated in *skn-1* mutants, a transcriptional regulator of the stress response and metabolic genes (Nhan et al., 2019). In addition, dietary restriction results in the upregulation of similar gene sets (Wu et al., 2019). These results together suggest that multiple types of lipid imbalance seem to impact immunity-linked gene expression and that these links may be conserved across species, as indicated by results in human cells cited above .

Exposure of *C. elegans* to bacterial pathogens stimulates the expression of a diverse set of genes, including antimicrobial peptides, enzymes for detoxifying xenobiotics, and neuromodulatory peptides to coordinate inter-organ defenses (Engelmann et al., 2011; Fletcher et al., 2019; Mallo et al., 2002; Troemel et al., 2006). However, many of the genes upregulated in response to either bacteria or fungi do not fall into these clearly

bioRxiv preprint doi: https://doi.org/10.1101/2021.11.16.468795; this version posted November 16, 2021. The copyright holder for this preprint (which was not certified by peer review) is the author/funder, who has granted bioRxiv a license to display the preprint in perpetuity. It is made available under aCC-BY-NC 4.0 International license.

79 defensive pathways (Estes et al., 2010) or have clear functional roles and are instead
80 defined by pathogen-responsive expression. In order to understand the relationship
81 between ILG regulation and changes in lipid levels, we compared lipidomics from *sams-*
82 *1* and *sbp-1* animals with results from a targeted RNAi screen for activation of the
83 immunity-linked reporter, p*sysm-1::GFP* (Shivers et al., 2009). We found that *sams-1*
84 *and sbp-1* knockdown animals both had broad changes in their lipidome. However,
85 fractionated *sbp-1* extracts showed low PC in the ER/Golgi fraction, as we previously
86 found in *sams-1* animals (Smulan et al., 2016). Our targeted RNAi screen argues that
87 synthesis of two lipid classes, PC and sphingomyelin (SM), increase p*sysm-1::GFP*
88 expression. In addition, RNAi of Golgi/ER transport regulators, including the GTPase
89 *arf-1/ARF1,* activated the immunity-linked reporter. Notably, some ILGs were also
90 upregulated after *arf-1*/ARF1 RNAi, suggesting that disrupting Golgi function regulates
91 immunity-linked genes. Finally, we find that RNAi of one ILG, *hpo-6*, disrupts the
92 trafficking of two secreted proteins. Taken together, our results suggest that some ILGs
93 act to balance the increased secretory load in pathogen-stimulated cells. While immune
94 function is critical for host defenses, immune activation in non-pathogenic conditions,
95 such as in metabolic disease, may have deleterious effects (Zmora et al., 2017). Thus,
96 our studies provide critical links between shifts in lipid metabolism and stimulation of
97 immunity-linked gene expression.
98

bioRxiv preprint doi: https://doi.org/10.1101/2021.11.16.468795; this version posted November 16, 2021. The copyright holder for this preprint (which was not certified by peer review) is the author/funder, who has granted bioRxiv a license to display the preprint in perpetuity. It is made available under aCC-BY-NC 4.0 International license.

Results

Gene set enrichment shows upregulation of pathogen-response genes in multiple models of membrane dysfunction

Levels of lipids within membranes are tightly monitored, and imbalances may induce cellular stress pathways that regulate genes to restore lipid ratios (Hotamisligil and Davis, 2016). We previously found that *sams-1*, *lpin-1,* and *sbp-1* are part of a feedback loop that responds to shifts in membrane PC levels and activates immunity-linked genes (Fig. 1A; Smulan et al., 2016; Walker et al., 2011). In order to test why immunity-linked genes are activated after disruption of lipid-synthesis regulators we first conducted a bioinformatics analysis using our recently developed *C. elegans* specific gene ontology tool, WormCat 2.0. This computational analysis allows combinatorial graphing of gene enrichment scores based on detailed annotation of all *C. elegans* genes (Higgins et al., 2021; Holdorf et al., 2019). This tool uses a nested annotation strategy (Category1/Category2/Category3) to provide broader or more detailed information on genome-wide datasets. In order to better characterize these ILGs, we used WormCat to directly compare genes upregulated in the *sams-1, sbp-1,* and *lpin-1* mutants (**Fig1A**). The Lee lab generously shared data of genes that are upregulated when *lpin-1* is knocked down in the absence of the stress-triggering glucose (Jung et al., 2020) **Table S1**). WormCat analysis indicates that all three knockdowns result in enrichment in the broad Category1(Cat1) STRESS RESPONSE category, and more specifically in Pathogen at the Cat2 level, similar to results from GO analysis (**Fig1A-C)**. Notably, the strongest enrichments at the Cat3 level were in STRESS RESPONSE: Pathogen: *other*. This category contains genes that increase upon pathogen exposure

bioRxiv preprint doi: https://doi.org/10.1101/2021.11.16.468795; this version posted November 16, 2021. The copyright holder for this preprint (which was not certified by peer review) is the author/funder, who has granted bioRxiv a license to display the preprint in perpetuity. It is made available under aCC-BY-NC 4.0 International license.

in *C. elegans* but do not have defined functions as antimicrobial peptides or within pathogen-stimulated signaling pathways such as MAPK signaling (Higgins et al., 2021; Holdorf et al., 2019). This class of genes is not explicitly defined by a traditional GO analysis. We also noted that the landscape of upregulated genes was complex, with STRESS RESPONSE: Detoxification enrichment scores increasing in both *sams-1* and *lpin-1* but not *sbp-1* (**Fig1B**). In addition, METABOLISM: Lipid was increased after *sams-1* and *lpin-1* RNAi (**Fig1B**). These data are consistent with our previous studies showing that SBP-1 transcriptional targets are upregulated in these animals (Walker et al., 2011), as are immunity-linked categories after SREBP-1 knockdown in human melanoma cell lines (Wu and Näär, 2019). Finally, WormCat analysis of microarray data from the Thibault lab (Koh et al., 2018) finds that STRESS RESPONSE: Pathogen is increased after knockdown of *pmt-2*, a methyltransferase essential in SAM-dependent PC production (**FigS1A**). Thus, genes linked to immunity are upregulated across a diverse set of lipid synthesis modulators in *C. elegans* and mammalian cells.

SBP-1/SREBP1 is a basic helix-loop-helix transcription factor required to express a suite of lipid metabolic genes, including *fat-7* in *C. elegans* and its ortholog SCD1 in mammals (HORTON et al., 2002; McKay et al., 2003). It is also necessary for the upregulation of *fat-7* in lipid-replete *sams-1(lof)* animals ((Walker et al., 2011), and **Fig1D**). Since SBP-1 upregulates lipid synthesis genes, we tested the possibility that it directly functions in ILG upregulation by using *sams-1(RNAi)* to increase the expression of multiple SBP-1 target genes (Walker et al., 2011). Whereas *fat-7* depends on *sbp-1* in both the control and *sams-1(RNAi)* background, *hpo-6* is expressed at high levels in

bioRxiv preprint doi: https://doi.org/10.1101/2021.11.16.468795; this version posted November 16, 2021. The copyright holder for this preprint (which was not certified by peer review) is the author/funder, who has granted bioRxiv a license to display the preprint in perpetuity. It is made available under aCC-BY-NC 4.0 International license.

both *sbp-1(RNAi)* and *sams-1(lof); sbp-1(RNAi)* animals (**Fig1D**). This suggests that the effects of SBP-1 on ILG upregulation are indirectly related to its function as a transcriptional regulator.

Many pathogen-responsive genes in *C. elegans* act downstream of signals from the p38/MAPK14 kinase PMK-1 (Troemel et al., 2006). In previous studies in *C .elegans*, we found that low PC in *sams-1(lof)* animals leads to constitutive phosphorylation of PMK-1 and that ILG induction was dependent on both PC and *pmk-1* (Ding et al., 2015). In order to confirm this effect in mammalian cells, we used siRNA to knock down the rate-limiting enzyme for PC production, *PCYT1,* in human hepatoma cells (**FigS1B**). We found that p38/MAPK14 phosphorylation is induced to levels similar to lipopolysaccharide (LPS). In *C. elegans*, knockdown of *sbp-1* also induces PMK-1 phosphorylation (**FigS1C**). Taken together, the results suggest that upregulation of ILGs in response to lipid perturbations may share regulatory link to pathogen-stimulated pathways.

Loss of sbp-1 decreases PC levels in ER/Golgi extracts

Immunity-linked gene expression and PMK-1 phosphorylation both occur after reduction in *sams-1* and *sbp-1*, although these genes act at different points in lipid synthesis regulation. Next, we sought to identify any shared signatures in the total lipidomes of these mutants by LC/MS. Because animals were lysed directly into lipid extraction buffer, levels were normalized to total lipid as in (Smulan et al., 2016). The entire lipidome was broadly altered in both cases, with 27% of lipid species showing significant

bioRxiv preprint doi: https://doi.org/10.1101/2021.11.16.468795; this version posted November 16, 2021. The copyright holder for this preprint (which was not certified by peer review) is the author/funder, who has granted bioRxiv a license to display the preprint in perpetuity. It is made available under aCC-BY-NC 4.0 International license.

168 changes in *sams-1(RNAi)* animals and 30% after *sbp-1(RNAi)* (**Fig2A, B; Table S2**).
169 We next examined lipid levels at the class and species level. As in our previous studies
170 (Cell 2011), *sams-1* animals showed lower PC and higher TAG (**Fig2C**), and we also
171 noted lower phosphatidylserine (PS) and SM levels in comparison to other lipid classes
172 (**Fig2C, FigS1C**). TAG was lower after *sbp-1* RNAi, as expected from previous studies
173 (Yang et al., 2006). We also found that while reductions in PC did not reach
174 significance, PE increased, and Cer levels dropped (**Fig2C, D**). In short, *sbp-1* RNAi
175 induces broad changes in the lipidome across multiple classes of lipids.
176
177 The properties of lipid classes can be altered when distributions of acyl chains change
178 significantly. We find that there are significant differences in the populations of species
179 within phospholipids (PC, phosphatidylethanolamine (PE), lyso-
180 phosphatidylethanolamine (LPE), and phosphatidylglycerol (PG), triglycerides (TAG),
181 diacylglycerides (DG), and sphingomyelins (SM) after *sams-1(RNAi)*. Changes in
182 species distribution in lipid classes after *sbp-1* RNAi were limited to TAG, lyso-
183 phosphatidylcholine (LPC), and ceramides (Cer) in agreement with previous studies
184 showing lower TAGs in *sbp-1(RNAi)* animals. We asked if *sams-1* and *sbp-1* RNAi
185 caused similar shifts in animals and found overlapping changes in 180 shared lipid
186 species (**TableS2**). 57 of these species were decreased in both, 17 increased in both,
187 and 102 lipid species changed in opposite directions out of 1405 total lipid species
188 detected. Lipid species diverged most strongly within the TG class, with increases in
189 *sams-1(RNAi)* animals and decreases after *sbp-1* RNAi (**TableS2**). This agreed with
190 total class levels. For lipid species that increased in both animals, PE species were the

bioRxiv preprint doi: https://doi.org/10.1101/2021.11.16.468795; this version posted November 16, 2021. The copyright holder for this preprint (which was not certified by peer review) is the author/funder, who has granted bioRxiv a license to display the preprint in perpetuity. It is made available under aCC-BY-NC 4.0 International license.

191 highest, with 15 changing at significant levels. 74 PC species changed in both *sams-1*
192 and *sbp-1* animals, with 35 decreasing in both (**TableS2**). Finally, three SM species
193 decreased in both animals. Thus, while *sams-1* or *sbp-1* knockdown each lead to broad
194 changes in the total lipidome, relatively few overlapping species changed in both
195 instances. Of those, PC species were the best represented among lipid species that
196 decreased upon knockdown of either *sams-1* or *sbp-1* in animals.
197
198 The total lipidome contains multiple organelles, including the plasma membrane,
199 mitochondria, nuclear membrane, and Golgi/ER. However, lipid ratios in specific
200 organelles may be reflective of particular functions; for example, we previously found
201 that PC ratios in ER/Golgi fractions were associated with activation of SBP-1 in *sams-1*
202 and *lpin-1* animals (Smulan et al., 2016). Therefore, we performed LC/MS lipidomics on
203 microsomes from *sbp-1(RNAi)* animals. Because the lipidomics was performed on
204 fractionated animals, we used total protein for normalization. We found a broader
205 fraction of the ER/Golgi lipidome was affected after *sbp-1(RNAi)* than in the total lipid
206 samples. Nearly 40% of lipid species were altered in these fractions (**Fig2E; Table S2**),
207 with significant changes in species across most classes (**FigS1C**). Similar to the
208 unfractionated extracts, levels of TAG and Cer decreased in the ER/Golgi (**Fig2F**).
209 Notably, significant ER/Golgi-specific decreases occurred in PC and DG (**Fig2F, G;**
210 **FigS1D**). This demonstrates that *sbp-1(RNAi)* has distinct effects on the ER/Golgi
211 membranes and shows decreases in PC levels at the sub-compartment level, similar to
212 *sams-1* RNAi.
213

bioRxiv preprint doi: https://doi.org/10.1101/2021.11.16.468795; this version posted November 16, 2021. The copyright holder for this preprint (which was not certified by peer review) is the author/funder, who has granted bioRxiv a license to display the preprint in perpetuity. It is made available under aCC-BY-NC 4.0 International license.

214 ***Targeted RNAi Screen Reveals roles for Ceramide/Sphingomyelin synthesis and***
215 ***COP I transport in immune gene expression***

216 Low PC levels are associated with ILG expression in *sams-1* (Ding et al., 2015) and
217 *pmt-2(RNAi)* animals (Koh et al., 2018). The low PC in the ER/Golgi compartment of
218 both *sams-1* (Smulan et al., 2016) and *sbp-1* RNAi animals suggests this could be a
219 shared signature linked to ILG upregulation. To understand how these lipids might act,
220 we next sought to identify genes important for ILG expression. We screened for
221 upregulation of an immune reporter, p*sysm-1*::GFP (Shivers et al., 2009), with an RNAi
222 sub-library that targets genes involved in complex lipid metabolism, lipid signaling and
223 selected ER/Golgi transport regulators. We previously used a lipid-function RNAi sub-
224 library to identify low-PC regulators of SBP-1/SREBP-1 (Smulan et al., 2016). Notably,
225 we constructed RNAi clones for genes not represented in the Arhinger or Orfeome RNAi
226 libraries. The resulting library includes all predicted phospholipases and enzymes for
227 synthesis of complex lipids (Smulan et al., 2016). For the current screen, we expanded
228 the sub-library to include more genes involved in ceramide/sphingomyelin synthesis and
229 confirmed all clone identities by sequencing. Thus, this library has a broader
230 representation of genes linked to complex lipid synthesis than the commercially
231 available RNAi libraries. p*sysm-1*::GFP is strongly induced by *sbp-1(RNAi)* (**Fig3A**) and
232 has been used by multiple labs as a robust marker for immune gene induction (Jeong et
233 al., 2017; Pender and Horvitz, 2018; Wu et al., 2019).
234
235 In order to identify genes in lipid synthesis important for ILG upregualion, we screened
236 this library in quadruplicate in p*sysm-1*::GFP animals and identified a list of 20

bioRxiv preprint doi: https://doi.org/10.1101/2021.11.16.468795; this version posted November 16, 2021. The copyright holder for this preprint (which was not certified by peer review) is the author/funder, who has granted bioRxiv a license to display the preprint in perpetuity. It is made available under aCC-BY-NC 4.0 International license.

237 candidates for retesting (**Fig3B; Table S3**). Retesting to identify the strongest
238 candidates occurred in 3 stages: visual rescreening (4X), imaging of candidates from
239 the rescreen, and qRT-PCR to assess changes in GFP expression. We also included
240 the *sbp-1* target genes *fat-5*, *fat-6,* and *fat-7* (McKay et al., 2003; Yang et al., 2006) in
241 the visual retesting. These genes are orthologs of mammalian Stearoyl CoA
242 desaturases (SCDs) (Watts and Browse, 2002) and can change membrane fluidity
243 (Bodhicharla et al., 2018; Ruiz et al., 2018) or induce lipid bilayer stress by changing
244 ratios of saturated/unsaturated acyl chains within lipid classes (Ho et al., 2018, 2020;
245 Koh et al., 2018).
246
247 Candidates from the targeted screen fell into two major groups. First, enzymes linked to
248 PC and SM synthesis were found (**Fig3C-G; FigS3A, B; TableS3**). This included two
249 isoforms of the rate-limiting enzyme for PC production, *pcyt-1,* and *sptl-1*, which initiates
250 the first committed step in sphingolipid synthesis. Thus, our genetic data supports the
251 notion that changes in PC or SMs are a shared signature linked to ILG activation in
252 *sams-1* and *sbp-1* RNAi animals. Notably, *fat-5, -6,* or *fat-7* RNAi, which would change
253 acyl chains saturation within each lipid class, had modest effects on the p*sysm-1*::GFP
254 immune reporter (**Fig3H, FigS3A, B; Table S3**), suggesting changes in membrane
255 fluidity downstream of these enzymes is not a major contributor to the immunity-linked
256 gene upregulation.
257
258 Second, genes involved in Golgi/ER trafficking activated the reporter in both strains
259 (**Fig3C, D; Fig43A, B; TableS3**). Golgi/ER trafficking genes included four genes

bioRxiv preprint doi: https://doi.org/10.1101/2021.11.16.468795; this version posted November 16, 2021. The copyright holder for this preprint (which was not certified by peer review) is the author/funder, who has granted bioRxiv a license to display the preprint in perpetuity. It is made available under aCC-BY-NC 4.0 International license.

forming the COPI complex (which also caused developmental delays) and ARF1 guanine activating factor (*agef-1*). The ARF-1 GTPase, a key regulator of these factors, was a false negative in the original screen, but strongly activated the reporter in the rescreening. (**Fig3I**; **Table S3**). The coatomer proteins work in a complex (Spang, 2002) and are required for viability (Fraser et al., 2000). Therefore, we chose one candidate, *copa-1,* and performed RNAi with diluted bacteria, allowing animals to develop fully. We found that the immune activation reporter was strongly expressed in the *copa-1* knockdown (**Fig3I**). Stimulation of the reporter after the loss of multiple parts of the COP I machinery and its key regulator *arf-1* strongly argues that ER/Golgi dynamics signal to induce immunity-linked genes.

The p*sysm-1*::GFP reporter represents a single gene in the immune response program. To more broadly survey ILGs in our screen validation, we used qRT-PCR with primers specific to the endogenous *sysm-1* gene, *irg-1, irg-2,* and *hpo-6*, and found robust activation of each of our candidate reporters after knockdown of *arf-1* or *copa-1*, but more modest effects with the SM genes or SCDs (**FigS4C-G)**. Integration of results from this targeted RNAi screen with our lipidomics studies shows overlap in two main areas, PC and SM synthesis, which are themselves connected. We previously linked changes in PC levels in *sams-1* microsomes to the inactivation of ARF-1, which drove proteolytic processing of SBP-1/SREBP-1 (Smulan et al., 2016). These results suggest that blocking ARF-1 function could also be linked to ILG activation.

Disruption of ER/Golgi activates immunity-linked genes

bioRxiv preprint doi: https://doi.org/10.1101/2021.11.16.468795; this version posted November 16, 2021. The copyright holder for this preprint (which was not certified by peer review) is the author/funder, who has granted bioRxiv a license to display the preprint in perpetuity. It is made available under aCC-BY-NC 4.0 International license.

The upregulation of *sysm-1* and other immune genes after *arf-1* RNAi prompted us to examine genome-wide changes in the transcriptome that could occur in response to the loss of ARF-1 function. Using RNA-seq, we found that 705 genes were significantly upregulated after *arf-1* RNAi (**Fig4A, FigS3A; Table S4**) and that 40% of these genes were also upregulated in *sams-1* or *sbp-1* RNAi animals (**FigS4A**). Downregulated genes in *sams-1, sbp-1,* or *arf-1* animals had low levels of overlap (**FigS4B**). WormCat gene set enrichment shows that STRESS RESPONSE: Pathogen: *Other* gene sets are significantly upregulated in *arf-1(RNAi)* animals as they are after *sbp-1, sams-1,* or *lpin-1* RNAi (**Fig4B**). Next, we examined WormCat enrichment within the genes that were shared between these three RNAi sets and found that shared genes retained strong enrichment for STRESS RESPONSE: Pathogen (**FigS4C-D**). Thus, *arf-1* GTPase knockdown causes similar or overlapping effects in immune gene expression to those seen after broad lipid disruption by *sbp-1* RNAi. Cycling of the ARF1 GTPase requires interaction with the Golgi membrane (Spang, 2002). In order to study the localization of ARF-1, we obtained a strain where endogenous ARF-1 is C-terminally tagged by CRISPR. Next, we asked if ARF-1 localization was altered in *sbp-1(RNAi)* animals by examining expression in the ARF-1::RFP animals. In intestinal cells, ARF-1::RFP formed a punctate pattern (**Fig4C**) similar to that of the Golgi ministacks characteristic of *C. elegans* cells (Broekhuis et al., 2013) (See also **Fig4D**). Strikingly, ARF-1::RFP appeared to form larger, more irregular punctae in *sbp-1(RNAi)* animals as well as having additional diffuse localization, similar to patterns seen with RNAi of the coatomer protein COPA-1 (**Fig4C**). This suggests that ARF-1 functions at the Golgi are altered in *sbp-1(RNAi)* animals.

bioRxiv preprint doi: https://doi.org/10.1101/2021.11.16.468795; this version posted November 16, 2021. The copyright holder for this preprint (which was not certified by peer review) is the author/funder, who has granted bioRxiv a license to display the preprint in perpetuity. It is made available under aCC-BY-NC 4.0 International license.

Loss of human ARF1 or blocking ARF1 cycling with the fungal toxin BrefeldinA disrupts Golgi integrity (Klausner et al., 1992). In addition, our previous studies found that lowering PC levels through RNAi of *sams-1* or knockdown of *PCYT1* (the rate-limiting enzyme for PC production) in mammalian cells blocked ARF1 GTPase activity and disrupted Golgi structure (Smulan et al., 2016; Walker et al., 2011). Because PC levels in *sbp-1(RNAi)* ER/Golgi fractions decreased (**Fig2C**) and ARF-1::RFP was mislocalized, we next examined Golgi structure in *sbp-1(RNAi)* animals using a reporter, MANS::GFP, driven by an intestinal reporter (Chen et al., 2006). MANS::GFP is a fusion of *aman-2* (alpha-mannosidase, a conserved Golgi specific protein) and marks the mini-Golgi stacks characteristic of *C. elegans* (Rolls et al., 2002). Consistent with previous studies (Ackema et al., 2013; Sato et al., 2006), knockdown of *arf-1* dramatically shifts the Golgi puncta to diffuse localization across the cytoplasm (**Fig4D**). *copa-1* RNAi also diminished Golgi stacks along with altering ARF-1::RFP localization (**Fig4C, D**). *sbp-1* knockdown affects Golgi structure, but results in a different pattern (**Fig4E**). Golgi stacks are more numerous and smaller with increases in diffuse cytoplasmic localization (**Fig4E**). Notably, *sptl-1(RNAi)* did not noticeably alter Golgi marked by MANS::GFP and ARF-1::RFP puncta were visible, suggesting that *sptl-1* knockdown may mediate effects on immune genes through and SM pathways through different cellular membranes. Taken together, we find that ARF-1 activity (Smulan et al., 2016) and localization (this study) can be affected by *sams-1* or *sbp-1* RNAi and that targeting *arf-1* or the coatomer components can activate ILGs. Thus, blocking or limiting ARF-1 function at the Golgi may be part of the signal to activate these genes.

bioRxiv preprint doi: https://doi.org/10.1101/2021.11.16.468795; this version posted November 16, 2021. The copyright holder for this preprint (which was not certified by peer review) is the author/funder, who has granted bioRxiv a license to display the preprint in perpetuity. It is made available under aCC-BY-NC 4.0 International license.

329

330 ***Immunity-linked gene upregulation in models of trafficking dysfunction***

331 The Golgi apparatus accepts proteins from the ER that are destined for secretion,
332 processing them by glycosylation before secretory vesicles are loaded (Boncompain
333 and Weigel, 2018). Stimulation of the innate immune system may significantly impact
334 trafficking load, as antimicrobial peptides are shuttled through the membrane trafficking
335 system (Taguchi and Mukai, 2019). Indeed activation of the ER stress response has
336 been noted in multiple systems when large numbers of proteins need to be produced
337 and secreted (Gardner et al., 2013). Interestingly, previous data suggest that induction
338 of membrane stress may also be a sensor of infection (Lamitina and Chevet, 2012).
339 Based on work by the Ewbank lab, they also suggested that some pathogen-response
340 genes act to support the trafficking of antimicrobial peptides (AMPs) (Couillault et al.,
341 2012; Lamitina and Chevet, 2012). We noted that the immunity-linked genes
342 upregulated at low PC are largely outside of the antimicrobial categories and are
343 comprised of gene sets defined by their shared expression upon pathogen exposure
344 rather than function (Estes et al., 2010; Holdorf et al., 2019). We hypothesized that
345 some of these genes might be responding to direct stress on the trafficking system.

346

347 To explore this idea, we turned to two commonly used systems for studying trafficking in
348 *C. elegans*, visualization of VIT-2::GFP (Grant and Sato, 2006) and *myo-3*::GFP (Fares
349 and Greenwald, 2001). *vit-2* is vitellogenin produced and secreted from intestinal cells
350 and taken up by the germline (Grant and Hirsh, 1999). *myo-3*::ssGFP has a signal
351 sequence on the fluorophore and is expressed in body wall muscle (Fares and

bioRxiv preprint doi: https://doi.org/10.1101/2021.11.16.468795; this version posted November 16, 2021. The copyright holder for this preprint (which was not certified by peer review) is the author/funder, who has granted bioRxiv a license to display the preprint in perpetuity. It is made available under aCC-BY-NC 4.0 International license.

Greenwald, 2001) Two published studies examine genome-wide mRNA expression patterns when *vit-2* is overexpressed or misregulated. First, we used WormCat to examine category enrichment data from germline-less *glp-1* mutants obtained by the Blackwell lab, where they showed that *vit-2*::GFP builds up near its production site in the intestines (Steinbaugh et al., 2015)and found strong enrichment patterns in STRESS RESPONSE: Pathogen: other (Fig5A). Next, we used WormCat to examine RNA-seq data from VIT-2::GFP (Singh and Aballay, 2017) overexpressing animals produced by the Aballay group and also fund increased stress response genes (**Fig5B).**

In order to more directly test the hypothesis that increased protein load could lead to activation of these ILGs, we compared two strains with a differing copy number of *vit-2*; RT130, made by microparticle bombardment and containing the GFP array in addition to wild type copies (Balklava et al., 2016) and BCN9071 which is a CRISPR-generated allele integrated into the endogenous locus (Rompay et al., 2015) (**Fig4E**). Van Rompay reported that total yolk protein levels were higher in strains harboring *vit-2*::GFP derived from RT130 (Rompay et al., 2015). Where we found by RT-PCR that GFP expression levels were also increased (**Fig4F**). Thus, increasing the amount of VIT-2::GFP produced was also associated with ILG upregulation.

We found that ILGs become upregulated in the absence of pathogen response when lipid levels become unbalanced, ARF-1 functions are compromised, or when protein production is increased. We next tested whether increased ILG expression was part of a response to help stimulate passage through the secretory pathway when trafficking

bioRxiv preprint doi: https://doi.org/10.1101/2021.11.16.468795; this version posted November 16, 2021. The copyright holder for this preprint (which was not certified by peer review) is the author/funder, who has granted bioRxiv a license to display the preprint in perpetuity. It is made available under aCC-BY-NC 4.0 International license.

load is high. One of the most strongly upregulated genes is *hpo-6*, which is not present in any of the commercially available RNAi libraries. To study its function more closely in this context, we made a cDNA construct to allow RNAi in VIT-2::GFP RT130 in wild type and *sams-1(lof)* animals (Ding et al., 2015). *hpo-6* was originally identified in a screen for genes whose loss increased sensitivity to a pore-forming toxin (Kao et al., 2011). It has a glycoprotein domain and may occur in membrane rafts (Rao et al., 2011), but has no apparent homology to human proteins . *hpo-6(RNAi)* causes a slight increase in VIT-2::GFP in wild-type animals (**Fig6S**). However, in the low PC *sams-1(lof)* background, VIT-2::GFP pooling and aggregation suggested a broad effect on trafficking patterns (**Fig6S)**. Yolk in *C. elegans* consists of both lipids and proteins (Perez and Lehner, 2019). Because low lipid levels in *sbp-1(RNAi)* animals makes results with VIT-2::GFP difficult to interpret, we used the *myo-3*::ssGFP reporter model (Fares and Greenwald, 2001), which expresses and secretes GFP in body wall muscle cells. We used this reporter to examine the effects of *hpo-6* on secretion when *sbp-1* function is reduced. First, we confirmed that knockdown of *arf-1* or *sbp-1* affected secretion of the reporter, finding broad pooling and aggregation after *arf-1(RNAi)* and aggregation with *sbp-1(RNAi)* (**Fig5H**). As in VIT-2::GFP, *hpo-6(RNAi)* had modest effects in the wild-type background, with the appearance of small aggregates. (**Fig5H**). In order to test the effects of blunting *hpo-6* upregulation in sbp-1 animals, we crossed *myo-3*::ssGFP into a strain harboring a hypomorphic *sbp-1* allele *sbp-1(ep79)* (Brock et al., 2006). We found that *hpo-6* knockdown increased the pooling and aggregation in *myo-3::ssGFP*; *sbp-1(ep79)* animals (**Fig5I**). This suggests that some of ILGs respond

bioRxiv preprint doi: https://doi.org/10.1101/2021.11.16.468795; this version posted November 16, 2021. The copyright holder for this preprint (which was not certified by peer review) is the author/funder, who has granted bioRxiv a license to display the preprint in perpetuity. It is made available under aCC-BY-NC 4.0 International license.

397 to changes in secretory function that could occur with lipid imbalance, trafficking load, or

398 pathogen exposure and support secretory function.

399

400

bioRxiv preprint doi: https://doi.org/10.1101/2021.11.16.468795; this version posted November 16, 2021. The copyright holder for this preprint (which was not certified by peer review) is the author/funder, who has granted bioRxiv a license to display the preprint in perpetuity. It is made available under aCC-BY-NC 4.0 International license.

401 ## Discussion

402 Cellular stress arises when essential functions are limited or become unbalanced.
403 Membranous organelles are sensitive to both changes in intrinsic protein activity or
404 alterations of lipids within their bilayers and elicit gene expression programs when
405 stressed. While some stress-responsive genes have clear functions, many genes are
406 defined solely as being responsive to specific stresses (Holdorf et al., 2019; Nadal et al.,
407 2011). It is striking that altering membrane lipids activates a gene expression program
408 shared with pathogen stress in both *C. elegans* (Ding et al., 2015; Ho et al., 2020; Jung
409 et al., 2020) and mammals (Wu and Näär, 2019). Mammalian SREBP-1a has also
410 been implicated as a regulator of innate immune gene expression in macrophages (Im
411 et al., 2011). The secretory pathway is relevant to both membrane stress and immune
412 function about might therefore be regulated by both responses. Membrane organelles
413 such as the ER and Golgi are part of a more extensive trafficking system where proteins
414 and lipids are created, modified, then sent to proper intercellular locations or secreted
415 (Yarwood et al., 2020). Innate immune responses challenge trafficking systems as
416 antimicrobial peptides are produced in mass in the ER, sent in lipid vesicles to the
417 Golgi, where many are glycosylated and then packaged into lipid vesicles for secretion
418 (Bednarska et al., 2017). For example, the *C. elegans* genome contains more than 300
419 genes that are produced in response to specific pathogens (Engelmann et al., 2011)
420 and share similarity to known antimicrobial effectors (Dierking et al., 2016). In addition,
421 pathogen-responses require an intact ER stress pathway to allow adjustment to the
422 increased trafficking load (Lamitina and Chevet, 2012; Richardson et al., 2010).
423

bioRxiv preprint doi: https://doi.org/10.1101/2021.11.16.468795; this version posted November 16, 2021. The copyright holder for this preprint (which was not certified by peer review) is the author/funder, who has granted bioRxiv a license to display the preprint in perpetuity. It is made available under aCC-BY-NC 4.0 International license.

The ER contains multiple pathways that respond to changes in proteostasis and lipid levels (Gardner et al., 2013). These processes are orchestrated by ER-intrinsic proteins that sense changes in protein folding or alterations in the lipid bilayer and have important roles in basal conditions, as well as when the secretory system is overloaded (Hotamisligil and Davis, 2016; Safra et al., 2013). ER-linked events are also important during pathogen exposure in *C. elegans*; changes in ribosomal function at the ER have a well-defined impact on pathogen responses (Dunbar et al., 2012; McEwan et al., 2012) and pathogen responses depend on ER stress pathways (Richardson et al., 2010; Tillman et al., 2018). Interestingly, the Lee lab also found that ILGs are upregulated when trafficking is inhibited through blocking glycosylation in the ER (Jeong et al., 2020). Other organelles in the secretory pathway, such as the Golgi, have their own stress sensors and response pathways (Machamer, 2015). Our results suggest that disruption of trafficking outside the ER by targeting ARF-1 in the Golgi can also initiate a stress response stimulating ILG induction.

Genes upregulated by pathogen exposure include both antimicrobial effectors and many genes of unknown function (Estes et al., 2010; Troemel et al., 2006). Notably, the ILGs enriched after membrane stress are primarily those of unknown function. Several lines of evidence prompted us to hypothesize that some of these genes might be part of a response linked to stress in membranes of the secretory pathway rather than a direct response to an extrinsic pathogen. First, the involvement of secretory organs was implicated by alterations in PC ratios in the ER/Golgi in both *sams-1* and *sbp-1* RNAi lipidomes. Second, our targeted RNAi screen for regulators of p*sysm-1::GFP* identified

bioRxiv preprint doi: https://doi.org/10.1101/2021.11.16.468795; this version posted November 16, 2021. The copyright holder for this preprint (which was not certified by peer review) is the author/funder, who has granted bioRxiv a license to display the preprint in perpetuity. It is made available under aCC-BY-NC 4.0 International license.

447 the *arf-1* GTPase and coatomer proteins, which are critical Golgi/ER transport.
448 Importantly, knockdown of *arf-1* was sufficient to induce ILG upregulation.
449 Strengthening this link between disruption of lipid levels and ARF-1 function, we also
450 found *sbp-1* RNAi altered ARF-1::RFP localization and Golgi morphology.
451
452 ARF-1 is a critical regulator of trafficking, coordinating retrograde traffic from the Golgi
453 to the ER and regulating secretory function in the trans-Golgi (Donaldson and Jackson,
454 2011). Cycling of ARF-1 GTPases depends on membrane localization of the ARF
455 GTPase, GEF, and GAP (GTPase activating protein) (Donaldson and Jackson, 2011).
456 We previously found that knockdown of PC synthesis enzymes blocked ARF1 cycling
457 and limited membrane association of the ARF GEF GBF1 in cultured human cells
458 (Smulan et al., 2016). This suggests low PC levels affect ARF1 activity by limiting the
459 ability of the GTPase, GEF, and GAP to associate at the Golgi membrane and initiate
460 GDP-GTP cycling. However, PC could be linked to ARF1 through other mechanisms.
461 ARF1 and phospholipase D (PLD) function have been linked by multiple labs (Riebeling
462 et al., 2009). PLD cleaves PC molecules to produce choline and phosphatidic acid,
463 which in turn stimulates vesicle formation (McDermott et al., 2004). This regulatory loop
464 requires PC, which is low in ER/Golgi membranes in *sams-1* and *sbp-1* RNAi animals.
465 DAG kinases, which could be stimulated by changes in DAGs in the *sbp-1* or *sams-*
466 *1(RNAi)* animals, can also affect ARF activity and trafficking (Huijbregts et al., 2000).
467 Finally, Protein Kinase D has an important role in maintaining Golgi structure, and its
468 ortholog has been linked to immunity in *C. elegans* (Malhotra and Campelo, 2011; Ren
469 et al., 2009). However, none of these components activated the p*sysm-1::GFP* reporter

bioRxiv preprint doi: https://doi.org/10.1101/2021.11.16.468795; this version posted November 16, 2021. The copyright holder for this preprint (which was not certified by peer review) is the author/funder, who has granted bioRxiv a license to display the preprint in perpetuity. It is made available under aCC-BY-NC 4.0 International license.

in our RNAi screen, suggesting they could be important in other regulatory contexts. Indeed, the breadth of change in the lipidomes after *sams-1* or *sbp-1* RNAi suggests that other inputs could link lipids and ILG expression. In addition, other cellular processes may also affect ILG expression either in basal conditions or during pathogen infection. For example, there is a complex relationship between pathogen infection, proteotoxic stress, and induction of ILGs (Reddy et al., 2017)

In conclusion, our data suggest that the ILG induction after both broad disruption in membrane lipids and pathogen exposure occurs because both processes stress the trafficking system. We also find that one the upregulated immune-linked genes, *hpo-6*, can facilitate trafficking function. Our results suggest ILG induction may represent a "multi-membrane" stress response encompassing the roles of both the ER and the Golgi in trafficking. Many mammalian studies on the effect of lipids on innate immune functions have focused on specific lipids as stimulators of signaling pathways (Barnett and Kagan, 2019). Taken together, these results suggest that levels of specific membrane lipids can initiate stress responses sensitive to trafficking defects, which could impact immune function as well as other secretion-dependent processes. Cells contain complex systems for managing stress in the initial organelle of the secretory process, the ER, which may respond to disturbances in protein synthesis, aggregation, or lipid imbalances with specific programs of gene expression (Costa-Mattioli and Walter, 2020; Hotamisligil and Davis, 2016). Thus, the expression of ILGs may reflect a broader stress response that affects multiple secretory organelles, as processes beyond translation and folding are affected.

bioRxiv preprint doi: https://doi.org/10.1101/2021.11.16.468795; this version posted November 16, 2021. The copyright holder for this preprint (which was not certified by peer review) is the author/funder, who has granted bioRxiv a license to display the preprint in perpetuity. It is made available under aCC-BY-NC 4.0 International license.

Experimental Model and Subject Details

C. elegans strains, RNAi constructs, and screening.

N2 (wild type), p*sysm-1::GFP,* and OP50 were obtained from the *Caenorhabditis* Genetics Center. CRISPR-tagged ARF-1, p*arf-1::arf-1::RFP,* was obtained from *In vivo* Biosystems and outcrossed 3 times. Normal growth media (NGM) was used unless otherwise noted. For RNAi, gravid adults were bleached onto NGM plates supplemented with ampicillin, tetracycline, and 6mM IPTG and 10X concentrated bacterial cultures. *C. elegans* were allowed to develop until the young adult stage before harvesting. Because of larval arrest, *copa-1* RNAi bacteria were diluted 1:10 in control RNAi bacteria before plating. For the RNAi screen, L1 larvae were plated into 96 well plates spotted with RNAi bacteria, and L4/young adults were scored from -3 to +3 with 0 as no change in 4 independent replicates.

Cell culture and siRNA transfection

HepG2 cells (ATCC, HB-8065) were grown in Minimum Essential Medium (Invitrogen) plus 10% FBS (Invitrogen), Glutamine (Invitrogen), and Sodium Pyruvate (Invitrogen). siRNA oligonucleotides transfections were done for 48 hours using Lipofectamine RNAiMAX Transfection Reagent (Invitrogen, 13778100), and cells were held for 16 hours in 1% Lipoprotein Deficient Serum (LDS) (Biomedical Technologies, BT907) and 25 µg/ml ALLN (Calbiochem) for 30 min prior to harvesting.

Immunoblotting:

bioRxiv preprint doi: https://doi.org/10.1101/2021.11.16.468795; this version posted November 16, 2021. The copyright holder for this preprint (which was not certified by peer review) is the author/funder, who has granted bioRxiv a license to display the preprint in perpetuity. It is made available under aCC-BY-NC 4.0 International license.

HepG2 cells: Syringe passage was used to lyse cells in High Salt RIPA (50 mM Tris, pH 7.4; 400 mM NaCl; 0.1% SDS; 0.5% NaDeoxycholate; 1% NP-40; 1 mM DTT, 2.5 µg/mL ALLN, Complete protease inhibitors (Roche). Invitrogen NuPage gels (4- 12%) were used for protein separation before transfer to nitrocellulose. Blots were probed with antibodies to phosphorylated p38 MAP Kinase, total p38, and STAT1 were used as a control. Immune complexes were visualized with Luminol Reagent (Millipore). Densitometry was performed by scanning the film, then analysis of pixel intensity with ImageJ software. Graphs show the average of at least three independent experiments with control values normalized to one.

C. elegans: Young adult animals were lysed by sonication in High Salt RIPA, and immunoblotting was performed as above.

Microscopy

P*sysm*-1::GFP *C. elegans* strains were grown until the L4/young adult transition, and images were acquired on a Zeiss Dissecting Scope with an Axiocam camera. ARF-1::RFP and MANS-1::GFP images were acquired on a Leica SPE confocal, and projections of confocal slices were produced. All images were taken at identical gain settings within experimental sets, and Adobe Photoshop was used for corrections to levels across experimental sets.

Lipidomics

bioRxiv preprint doi: https://doi.org/10.1101/2021.11.16.468795; this version posted November 16, 2021. The copyright holder for this preprint (which was not certified by peer review) is the author/funder, who has granted bioRxiv a license to display the preprint in perpetuity. It is made available under aCC-BY-NC 4.0 International license.

C. elegans total and microsomal lipidomics, including fractionation protocols, were performed at the Whitehead Metabolomics core as in Smulan et al. 2016. Statistical analysis was performed in Graphpad prism.

Gene expression analysis

Lysis of young adult *C. elegans* was performed in 0.5% SDS, 5% β-ME, 10 mM EDTA, 10 mM Tris-HCl ph7.4, 0.5 mg/ml Proteinase K, before purification of RNA by TRI-Reagent (Sigma). cDNA was produced with Transcriptor First-strand cDNA kits (Roche), and RT-PCR was performed using Kappa SYBR Green 2X Mastermix.

RNA for sequencing was purified using RNAeasy columns (Qiagen). RNA sequencing (including library construction was performed by BGI (Hong Kong). Reads were analyzed through the Dolphin analysis platform (https://dolphin.umassmed.edu/), using DeSeq to identify differentially expressed genes (Yukselen et al., 2020). Gene set enrichment was performed using WormCat (www.wormcat.com) (Holdorf et al., 2019).

bioRxiv preprint doi: https://doi.org/10.1101/2021.11.16.468795; this version posted November 16, 2021. The copyright holder for this preprint (which was not certified by peer review) is the author/funder, who has granted bioRxiv a license to display the preprint in perpetuity. It is made available under aCC-BY-NC 4.0 International license.

Acknowledgments

We would like acknowledge Drs. Seung-Jae Lee, Sujeong Kwon (Korea Advanced Institute of Science and Technology) for providing the *lpin-1* RNA seq data. We would also like to thank Drs. Seung-Jae Lee, Emily Troemel (USD) and members of the Walker lab for comments on the manuscript as well as Dr. Marian Walhout (UMASS Chan School of Medicine) for helpful discussion. We would like to acknowledge Wei Ding for technical support and Caroline Lewis (MIT) for metabolomics screening at the Whitehead Metabolomics core. We also thank Life Science Editors and Dr. Sabbi Lall for manuscript editing. Funding was from the NIA at the NIH: R01AG053355 and R56AG068670. Some strains were provided by the CGC, which is funded by the NIH Office of Research Infrastructure Programs (P40 OD010440).

Author Contributions

Conceptualization; AKW, CMW, LJS

Verification: AKW, CMW, LJS

Formal Analysis: AKW, CMW, LJS

Investigation: AKW, CMW, LJS, DL, MF

Resources: AKW

Data Curation: AKW

Writing: AKW

Writing/Editing: AKW, CMW, LJS,

Visualization: AKW

bioRxiv preprint doi: https://doi.org/10.1101/2021.11.16.468795; this version posted November 16, 2021. The copyright holder for this preprint (which was not certified by peer review) is the author/funder, who has granted bioRxiv a license to display the preprint in perpetuity. It is made available under aCC-BY-NC 4.0 International license.

Supervision: AKW

Funding: AKW

Declaration of Interests

The authors declare no competing interests

bioRxiv preprint doi: https://doi.org/10.1101/2021.11.16.468795; this version posted November 16, 2021. The copyright holder for this preprint (which was not certified by peer review) is the author/funder, who has granted bioRxiv a license to display the preprint in perpetuity. It is made available under aCC-BY-NC 4.0 International license.

Figure Legends

Figure 1: Upregulation of immunity-linked genes occurs downstream of multiple types of membrane lipid disruption. WormCat gene set enrichment shows STRESS RESPONSE (**A**) and STRESS RESPONSE: Pathogen (**B**) are upregulated in *lpin-1* RNAi animals, as in *sams-1* and *sbp-1(RNAi)* animals (Ding et al., 2015). Legend is in **C**. qRT-PCR shows that upregulation of an immunity-linked gene, *hpo-6*, in *sams-1(lof)* animals is not dependent on *sbp-1* (**D**).

Figure 2: Broad lipidomic changes in total and microsomal lipid compartments after *sams-1* or *sbp-1* RNAi. LC/MS lipidomics show that nearly a third of total lipid species change after *sams-1* or *sbp-1* RNAi (**A, B**). Significant changes in major lipid classes are mostly distinct in *sams-1* and *sbp-1* RNAi (**C, D**). See also **Figure S1** (**B, D**) for lipid species distributions and additional lipid class analysis. The microsomal (ER/Golgi) lipidome is also broadly altered after *sbp-1 RNAi* (**E**) and shows changes in different lipid classes than in the total lipidome (**F, G**). Error bars show standard deviation. Lipid class data is calculated by students T-Test. See Figure S1 for lipid species distributions and additional lipid class analysis.

Figure 3: Targeted RNAi screen reveals candidates linked to Golgi/ER trafficking and ceramide/sphingomyelin synthesis impact immunity gene expression. (**A**) Immune gene reporter p*sysm-1*::GFP is increased after *sbp-1* RNAi. (**B**) Screen schematic. (**C**) Schematic showing RNAi library coverage and screen candidates. Epifluorescence imaging showing validation of reporter activity after RNAi of lipid PC

bioRxiv preprint doi: https://doi.org/10.1101/2021.11.16.468795; this version posted November 16, 2021. The copyright holder for this preprint (which was not certified by peer review) is the author/funder, who has granted bioRxiv a license to display the preprint in perpetuity. It is made available under aCC-BY-NC 4.0 International license.

617 synthesis genes (**D**), SM synthesis genes (**E**) and the SCD *fat-7* (**F**). Epifluorescence
618 images showing GFP levels after RNAi of the *arf-1* GTPase or coatomer component
619 *copa-1* (**I**). Because of poor larval development, bacterial for *copa-1* RNAi was diluted
620 to 1:10. **J**. Epifluorescence images showing GFP levels genes linked to Golgi function.
621 For qRT-PCR, see **Figure S4.**
622
623 **Figure 4: Disruption of Golgi/ER trafficking increases expression of immunity-**
624 **related genes. A.** Scatter plot shows changes in gene expression after *arf-1* RNAi. **B.**
625 WormCat gene set enrichment chart shows an increase in stress response and
626 pathogen linked genes. **C.** Confocal projections of CRISPR tagged ARF-1::RFP reveal
627 that that Golgi-specific pattern is disrupted after *sbp-1* RNAi. Scale bar is 10 microns.
628 **D**. Confocal projections of the *C. elegans* Golgi marker MANS::GFP (Chen et al., 2006)
629 in Control, *sbp-1, arf-1,* and *copa-1 (1:10)* RNAi intestines. Scale bar is 10 microns.
630
631 **Figure 5: Immunity-linked genes are linked to trafficking disruption.** WormCat
632 gene enrichment of upregulated genes from *glp-1*(AA2735) (Steinbaugh et al., 2015)
633 and *vit-2(ac3)* compared to SJ4005 (Singh and Aballay, 2017)for Category 1 (**A**) and
634 Category 2 (**B**). Legend is in **C**. qRT-PCR comparing gene expression in wild type,
635 single copy *vit-2::GFP* (BCN9071, s) or multi copy (RT130, m) animals. **D** and **E** show
636 increase in GFP or *vit-2*. Immune response genes are shown in **F-I**. **J.** Confocal
637 images of body wall muscle cells expressing of the secretion marker *myo-3*::ssGFP. **K**.
638 Body wall muscle cells in imaged by confocal microscopy in *myo-3*::ssGFP; *sbp-1(ep79)*
639 animals.

bioRxiv preprint doi: https://doi.org/10.1101/2021.11.16.468795; this version posted November 16, 2021. The copyright holder for this preprint (which was not certified by peer review) is the author/funder, who has granted bioRxiv a license to display the preprint in perpetuity. It is made available under aCC-BY-NC 4.0 International license.

Supplemental information

Figure S1: Activation of Stress response pathways when PC synthesis is disrupted. A. WormCat analysis of microarray data from Koh, et al. 2018. **B.** The p38 MAP kinase MAPK14 is phosphorylated after siRNA of *PCYT1* in human hepatoma cells. **C.** Constitutive phosphorylation of the *C. elegans* MAPK14 ortholog, PMK-1, occurs after both *sams-1* and *sbp-1(RNAi)*.

Figure S2: Broad lipidomic changes in total and microsomal lipid compartments after *sams-1* or *sbp-1* RNAi. **A**. Schematic showing effects of PC producing pathways on ARF-1. Tables showing numbers lipid species within each class in the total lipidome (**B**) or ER/Golgi lipidome in *sbp-1(RNAi)* animals (**D**). Green boxes denote classes in which the distribution of the species within each RNAi significantly differed from controls using the Wilcoxen test for non-parametric data. Levels of lipid classes in total *sams-1* or *sbp-1* total lipidomics (**C**) or *sbp-1* ER/Golgi lipidomics (**E**).

Figure S3: Candidates from lipid sub-library RNAi screen. Table showing candidates from quadruplicate screening of the RNAi sub-library along with other genes selected as controls for the rescreen.

Figure S4: Regulation of immunity-linked genes in conditions of membrane disruption. qRT PCR quantitating GFP upregulation after knockdown of Golgi trafficking regulators **(A)** or lipid synthesis genes **(B)**. qRT-PCR from *psysm-1*::GFP (A-

bioRxiv preprint doi: https://doi.org/10.1101/2021.11.16.468795; this version posted November 16, 2021. The copyright holder for this preprint (which was not certified by peer review) is the author/funder, who has granted bioRxiv a license to display the preprint in perpetuity. It is made available under aCC-BY-NC 4.0 International license.

H) or p*sysm-1*::GFP; *sbp-1(ep79)* (I-K) shows effects of disrupting *arf-1* or membrane lipids on ILGs. Error bars show standard deviation.

Figure S5: Shared upregulation of immunity linked genes in *sams-1, sbp-1* and *arf-1* transcriptomic studies. Venn diagrams showing limited overlap of up- (A) or downregulated (**B**) genes after *sbp-1, sams-1* or *arf-1* RNAi. **C-D.** WormCat analysis comparing overlapping gene sets from *arf-1, sbp-1* and *sams-1* upregulated genes. Data for *arf-1* alone is the same as **Figure 4B**. Legend is in **E**. Confocal micrographs showing minimal changes after *sptl-1* RNAi in of MANS::GFP (**F**) or ARF-1::RFP (**G**). Bar show 10 microns.

Figure S6: Reduction in *hpo-6* exacerbates *sams-1(lof)* trafficking defects. Confocal projections of *C. elegans* intestinal cells expressing *vit-2*::GFP (RT130) in wild type or *sams-1(lof)* backgrounds.

Table S1: Transcriptomics and gene set enrichment from *lpin-1(RNAi)* animals. 2 fold upregulated genes in *lpin-1(RNAi)* animals. Gene set enrichment was performed using WormCat (Holdorf et al., 2019).

Table S2: **Total lipidomics of *sams-1* and *sbp-1(RNAi)* animals and microsomal lipidomics of *sbp-1(RNAi)* adults.** Datasets from two lipidomic studies. The first is LCMS data normalized to total lipids compared between Control, *sbp-1,* and *sams-1*(*RNAi)* adults. Tabs are labeled sams_sbp_Lipid class. The second dataset contains

bioRxiv preprint doi: https://doi.org/10.1101/2021.11.16.468795; this version posted November 16, 2021. The copyright holder for this preprint (which was not certified by peer review) is the author/funder, who has granted bioRxiv a license to display the preprint in perpetuity. It is made available under aCC-BY-NC 4.0 International license.

LCMS from Control and *sbp-1(RNAi)* microsome preps from adult animals. Significance of fold changes in individual lipids determined by students T-test.

Table S3: Results from the screen of the "lipid sub-library." Tabs 1 and 2 contain averaged results from quadruplicate screening of *sysm-1*::GFP or *sysm-1::GFP; sbp-1(ep79)*. The secondary screen contains averages from candidates selected from the first screen, plus *fat-5, fat-6,* and *fat-7* as additional test RNAis. The secondary screen was conducted in quadruplicate. ND is not done.

Table S4: Transcriptomic responses to trafficking disruption. RNAseq from control vs. *arf-1/arf-1.2(RNAi)* animals (arf_1_all, arf_2Xup) and gene set enrichment analysis produced in WormCat for Category 1, Category2 and Category3). WormCat analysis of *vit-2*::GFP (Singh and Aballay, 2017)and *glp-1* (Steinbaugh et al., 2015) datasets.

bioRxiv preprint doi: https://doi.org/10.1101/2021.11.16.468795; this version posted November 16, 2021. The copyright holder for this preprint (which was not certified by peer review) is the author/funder, who has granted bioRxiv a license to display the preprint in perpetuity. It is made available under aCC-BY-NC 4.0 International license.

699 # References

700

701 Ackema, K.B., Sauder, U., Solinger, J.A., and Spang, A. (2013). The ArfGEF GBF-1 Is
702 Required for ER Structure, Secretion and Endocytic Transport in *C. elegans*. Plos One
703 *8*, e67076.

704 Aramburu, J., Ortells, M.C., Tejedor, S., Buxadé, M., and López-Rodríguez, C. (2014).
705 Transcriptional regulation of the stress response by mTOR. Sci Signal *7*, re2–re2.

706 Balklava, Z., Rathnakumar, N.D., Vashist, S., Schweinsberg, P.J., and Grant, B.D.
707 (2016). Linking Gene Expression in the Intestine to Production of Gametes Through the
708 Phosphate Transporter PITR-1 in *Caenorhabditis elegans*. Genetics *204*, 153 162.

709 Barnett, K.C., and Kagan, J.C. (2019). Lipids that directly regulate innate immune signal
710 transduction. Innate Immun *26*, 4–14.

711 Bednarska, N.G., Wren, B.W., and Willcocks, S.J. (2017). The importance of the
712 glycosylation of antimicrobial peptides: natural and synthetic approaches. Drug Discov
713 Today *22*, 919–926.

714 Bodhicharla, R., Devkota, R., Ruiz, M., and Pilon, M. (2018). Membrane Fluidity Is
715 Regulated Cell Non-autonomously by *Caenorhabditis elegans* PAQR-2 and Its
716 Mammalian Homolog AdipoR2. Genetics *210*, 189 201.

717 Boncompain, G., and Weigel, A.V. (2018). Transport and sorting in the Golgi complex:
718 multiple mechanisms sort diverse cargo. Curr Opin Cell Biol *50*, 94–101.

719 Brock, T.J., Browse, J., and Watts, J.L. (2006). Genetic Regulation of Unsaturated Fatty
720 Acid Composition in *C. elegans*. Plos Genet *2*, e108.

721 Broekhuis, J.R., Rademakers, S., Burghoorn, J., and Jansen, G. (2013). SQL-1,
722 homologue of the Golgi protein GMAP210, modulates intraflagellar transport in *C.*
723 *elegans*. J Cell Sci *126*, 1785–1795.

724 Chen, C.C.-H., Schweinsberg, P.J., Vashist, S., Mareiniss, D.P., Lambie, E.J., and
725 Grant, B.D. (2006). RAB-10 Is Required for Endocytic Recycling in the *Caenorhabditis*
726 *elegans* Intestine. Mol Biol Cell *17*, 1286 1297.

727 Costa-Mattioli, M., and Walter, P. (2020). The integrated stress response: From
728 mechanism to disease. Science *368*, eaat5314.

729 Couillault, C., Fourquet, P., Pophillat, M., and Ewbank, J.J. (2012). A UPR-independent
730 infection-specific role for a BiP/GRP78 protein in the control of antimicrobial peptide
731 expression in *C. elegans* epidermis. Virulence *3*, 299 308.

bioRxiv preprint doi: https://doi.org/10.1101/2021.11.16.468795; this version posted November 16, 2021. The copyright holder for this preprint (which was not certified by peer review) is the author/funder, who has granted bioRxiv a license to display the preprint in perpetuity. It is made available under aCC-BY-NC 4.0 International license.

Dierking, K., Yang, W., and Schulenburg, H. (2016). Antimicrobial effectors in the nematode *Caenorhabditis elegans*: an outgroup to the Arthropoda. Philosophical Transactions Royal Soc B Biological Sci *371*, 20150299.

Ding, W., Smulan, L.J., Hou, N.S., Taubert, S., Watts, J.L., and Walker, A.K. (2015). s-Adenosylmethionine Levels Govern Innate Immunity through Distinct Methylation-Dependent Pathways. Cell Metab *22*, 633 645.

Donaldson, J.G., and Jackson, C.L. (2011). ARF family G proteins and their regulators: roles in membrane transport, development and disease. Nat Rev Mol Cell Bio *12*, 362 375.

Dunbar, T.L., Yan, Z., Balla, K.M., Smelkinson, M.G., and Troemel, E.R. (2012). *C. elegans* detects pathogen-induced translational inhibition to activate immune signaling. Cell Host Microbe *11*, 375 386.

Engelmann, I., Griffon, A., Tichit, L., Montañana-Sanchis, F., Wang, G., Reinke, V., Waterston, R.H., Hillier, L.W., and Ewbank, J.J. (2011). A Comprehensive Analysis of Gene Expression Changes Provoked by Bacterial and Fungal Infection in *C. elegans*. Plos One *6*, e19055.

Estes, K.A., Dunbar, T.L., Powell, J.R., Ausubel, F.M., and Troemel, E.R. (2010). bZIP transcription factor *zip-2* mediates an early response to Pseudomonas aeruginosa infection in *Caenorhabditis elegans*. Proc National Acad Sci *107*, 2153 2158.

Fares, H., and Greenwald, I. (2001). Genetic Analysis of Endocytosis in *Caenorhabditis elegans* : Coelomocyte Uptake Defective Mutants. Genetics *159*, 133–145.

Fletcher, M., Tillman, E.J., Butty, V.L., Levine, S.S., and Kim, D.H. (2019). Global transcriptional regulation of innate immunity by ATF-7 in *C. elegans*. Plos Genet *15*, e1007830.

Fraser, A.G., Kamath, R.S., Zipperlen, P., Martinez-Campos, M., Sohrmann, M., and Ahringer, J. (2000). Functional genomic analysis of *C. elegans* chromosome I by systematic RNA interference. Nature *408*, 325–330.

Gardner, B.M., Pincus, D., Gotthardt, K., Gallagher, C.M., and Walter, P. (2013). Endoplasmic Reticulum Stress Sensing in the Unfolded Protein Response. Csh Perspect Biol *5*, a013169.

Gianfrancesco, M.A., Paquot, N., Piette, J., and Legrand-Poels, S. (2018). Lipid bilayer stress in obesity-linked inflammatory and metabolic disorders. Biochem Pharmacol *153*, 168–183.

Grant, B., and Hirsh, D. (1999). Receptor-mediated endocytosis in the *Caenorhabditis elegans* oocyte. Mol Biol Cell *10*, 4311 4326.

bioRxiv preprint doi: https://doi.org/10.1101/2021.11.16.468795; this version posted November 16, 2021. The copyright holder for this preprint (which was not certified by peer review) is the author/funder, who has granted bioRxiv a license to display the preprint in perpetuity. It is made available under aCC-BY-NC 4.0 International license.

767 Grant, B.D., and Sato, M. (2006). Intracellular trafficking. Wormbook Online Rev C
768 Elegans Biology 1–9.

769 Halbleib, K., Pesek, K., Covino, R., Hofbauer, H.F., Wunnicke, D., Hänelt, I., Hummer,
770 G., and Ernst, R. (2017). Activation of the Unfolded Protein Response by Lipid Bilayer
771 Stress. Mol Cell *67*, 673 684.e8.

772 Higgins, D.P., Weisman, C.M., Lui, D.S., D'Agostino, F.A., and Walker, A.K. (2021).
773 WormCat 2.0 defines characteristics and conservation of poorly annotated genes in
774 Caenorhabditis elegans. Biorxiv. https://doi.org/10.1101/2021.11.11.467968

775 Ho, N., Xu, C., and Thibault, G. (2018). From the unfolded protein response to
776 metabolic diseases – lipids under the spotlight. J Cell Sci *131*, jcs199307.

777 Ho, N., Yap, W.S., Xu, J., Wu, H., Koh, J.H., Goh, W.W.B., George, B., Chong, S.C.,
778 Taubert, S., and Thibault, G. (2020). Stress sensor Ire1 deploys a divergent
779 transcriptional program in response to lipid bilayer stress. J Cell Biol *219*.

780 Holdorf, A.D., Higgins, D.P., Hart, A.C., Boag, P.R., Pazour, G.J., Walhout, A.J.M., and
781 Walker, A.K. (2019). WormCat: An Online Tool for Annotation and Visualization of
782 *Caenorhabditis elegans* Genome-Scale Data. Genetics genetics.302919.2019.

783 HORTON, J.D., GOLDSTEIN, J.L., and BROWN, M.S. (2002). SREBPs: Transcriptional
784 Mediators of Lipid Homeostasis. Cold Spring Harb Sym *67*, 491–498.

785 Hotamisligil, G.S., and Davis, R.J. (2016). Cell Signaling and Stress Responses. Csh
786 Perspect Biol *8*, a006072.

787 Huijbregts, R.P.H., Topalof, L., and Bankaitis, V.A. (2000). Lipid Metabolism and
788 Regulation of Membrane Trafficking. Traffic *1*, 195–202.

789 Im, S.-S., Yousef, L., Blaschitz, C., Liu, J.Z., Edwards, R.A., Young, S.G., Raffatellu, M.,
790 and Osborne, T.F. (2011). Linking Lipid Metabolism to the Innate Immune Response in
791 Macrophages through Sterol Regulatory Element Binding Protein-1a. Cell Metab *13*,
792 540 549.

793 Jeong, D., Lee, D., Hwang, S., Lee, Y., Lee, J., Seo, M., Hwang, W., Seo, K., Hwang,
794 A.B., Artan, M., et al. (2017). Mitochondrial chaperone HSP-60 regulates anti-bacterial
795 immunity via p38 MAP kinase signaling. Embo J *36*, 1046–1065.

796 Jeong, D.-E., Lee, Y., Ham, S., Lee, D., Kwon, S., Park, H.-E.H., Hwang, S.-Y., Yoo, J.-
797 Y., Roh, T.-Y., and Lee, S.-J.V. (2020). Inhibition of the oligosaccharyl transferase in
798 *Caenorhabditis elegans* that compromises ER proteostasis suppresses p38-dependent
799 protection against pathogenic bacteria. Plos Genet *16*, e1008617.

bioRxiv preprint doi: https://doi.org/10.1101/2021.11.16.468795; this version posted November 16, 2021. The copyright holder for this preprint (which was not certified by peer review) is the author/funder, who has granted bioRxiv a license to display the preprint in perpetuity. It is made available under aCC-BY-NC 4.0 International license.

Jung, Y., Kwon, S., Ham, S., Lee, D., Park, H.H., Yamaoka, Y., Jeong, D., Artan, M., Altintas, O., Park, S., et al. (2020). *Caenorhabditis elegans* Lipin 1 moderates the lifespan-shortening effects of dietary glucose by maintaining ω-6 polyunsaturated fatty acids. Aging Cell *19*.

Kao, C.-Y., Los, F.C.O., Huffman, D.L., Wachi, S., Kloft, N., Husmann, M., Karabrahimi, V., Schwartz, J.-L., Bellier, A., Ha, C., et al. (2011). Global Functional Analyses of Cellular Responses to Pore-Forming Toxins. Plos Pathog *7*, e1001314.

Klausner, R.D., Donaldson, J.G., and Lippincott-Schwartz, J. (1992). Brefeldin A: insights into the control of membrane traffic and organelle structure. The Journal of Cell Biology *116*, 1071 1080.

Koh, J.H., Wang, L., Beaudoin-Chabot, C., and Thibault, G. (2018). Lipid bilayer stress-activated IRE-1 modulates autophagy during endoplasmic reticulum stress. J Cell Sci *131*, jcs217992.

Lamitina, T., and Chevet, E. (2012). To UPR… and beyond!: A new role for a BiP/GRP78 protein in the control of antimicrobial peptide expression in *C. elegans* epidermis. Virulence *3*, 238–240.

Machamer, C.E. (2015). The Golgi complex in stress and death. Front Neurosci-Switz *9*, 421.

Malhotra, V., and Campelo, F. (2011). PKD Regulates Membrane Fission to Generate TGN to Cell Surface Transport Carriers. Csh Perspect Biol *3*, a005280 a005280.

Mallo, G.V., Kurz, C.L., Couillault, C., Pujol, N., Granjeaud, S., Kohara, Y., and Ewbank, J.J. (2002). Inducible Antibacterial Defense System in *C. elegans*. Curr Biol *12*, 1209–1214.

McDermott, M., Wakelam, M.J.O., and Morris, A.J. (2004). Phospholipase D. Biochem Cell Biol *82*, 225–253.

McEwan, D.L., Kirienko, N.V., and Ausubel, F.M. (2012). Host translational inhibition by Pseudomonas aeruginosa Exotoxin A Triggers an immune response in *Caenorhabditis elegans*. Cell Host Microbe *11*, 364 374.

McKay, R.M., McKay, J.P., Avery, L., and Graff, J.M. (2003). *C. elegans* A Model for Exploring the Genetics of Fat Storage. Dev Cell *4*, 131–142.

Nadal, E. de, Ammerer, G., and Posas, F. (2011). Controlling gene expression in response to stress. Nat Rev Genet *12*, 833–845.

Nhan, J.D., Turner, C.D., Anderson, S.M., Yen, C.-A., Dalton, H.M., Cheesman, H.K., Ruter, D.L., Naresh, N.U., Haynes, C.M., Soukas, A.A., et al. (2019). Redirection of

bioRxiv preprint doi: https://doi.org/10.1101/2021.11.16.468795; this version posted November 16, 2021. The copyright holder for this preprint (which was not certified by peer review) is the author/funder, who has granted bioRxiv a license to display the preprint in perpetuity. It is made available under aCC-BY-NC 4.0 International license.

834 SKN-1 abates the negative metabolic outcomes of a perceived pathogen infection. Proc
835 National Acad Sci *116*, 22322–22330.

836 Pender, C.L., and Horvitz, H.R. (2018). Hypoxia-inducible factor cell non-autonomously
837 regulates *C. elegans* stress responses and behavior via a nuclear receptor. Elife *7*,
838 e36828.

839 Perez, M.F., and Lehner, B. (2019). Vitellogenins - Yolk Gene Function and Regulation
840 in *Caenorhabditis elegans*. Front Physiol *10*, 1067.

841 Radanović, T., Reinhard, J., Ballweg, S., Pesek, K., and Ernst, R. (2018). An Emerging
842 Group of Membrane Property Sensors Controls the Physical State of Organellar
843 Membranes to Maintain Their Identity. Bioessays *40*, 1700250.

844 Rao, W., Isaac, R.E., and Keen, J.N. (2011). An analysis of the *Caenorhabditis elegans*
845 lipid raft proteome using geLC-MS/MS. J Proteomics *74*, 242 253.

846 Reddy, K.C., Dror, T., Sowa, J.N., Panek, J., Chen, K., Lim, E.S., Wang, D., and
847 Troemel, E.R. (2017). An Intracellular Pathogen Response Pathway Promotes
848 Proteostasis in C. elegans. Curr Biol *27*.

849 Ren, M., Feng, H., Fu, Y., Land, M., and Rubin, C.S. (2009). Protein Kinase D Is an
850 Essential Regulator of C. elegans Innate Immunity. Immunity *30*, 521–532.

851 Richardson, C.E., Kooistra, T., and Kim, D.H. (2010). An essential role for XBP-1 in host
852 protection against immune activation in *C. elegans*. Nature *463*, 1092 1095.

853 Riebeling, C., Morris, A.J., and Shields, D. (2009). Phospholipase D in the Golgi
854 apparatus. Biochimica Et Biophysica Acta Bba - Mol Cell Biology Lipids *1791*, 876 880.

855 Rolls, M.M., Hall, D.H., Victor, M., Stelzer, E.H.K., and Rapoport, T.A. (2002). Targeting
856 of Rough Endoplasmic Reticulum Membrane Proteins and Ribosomes in Invertebrate
857 Neurons. Mol Biol Cell *13*, 1778–1791.

858 Rompay, L.V., Borghgraef, C., Beets, I., Caers, J., and Temmerman, L. (2015). New
859 genetic regulators question relevance of abundant yolk protein production in *C. elegans*.
860 Sci Rep-Uk *5*, 1 16.

861 Ruiz, M., Bodhicharla, R., Svensk, E., Devkota, R., Busayavalasa, K., Palmgren, H.,
862 Ståhlman, M., Boren, J., and Pilon, M. (2018). Membrane fluidity is regulated by the C.
863 elegans transmembrane protein FLD-1 and its human homologs TLCD1/2. Elife *7*,
864 1309.

865 Safra, M., Ben-Hamo, S., Kenyon, C., and Henis-Korenblit, S. (2013). The *ire-1* ER
866 stress-response pathway is required for normal secretory-protein metabolism in *C.*
867 *elegans*. J Cell Sci *126*, 4136–4146.

bioRxiv preprint doi: https://doi.org/10.1101/2021.11.16.468795; this version posted November 16, 2021. The copyright holder for this preprint (which was not certified by peer review) is the author/funder, who has granted bioRxiv a license to display the preprint in perpetuity. It is made available under aCC-BY-NC 4.0 International license.

868 Sato, K., Sato, M., Audhya, A., Oegema, K., Schweinsberg, P., and Grant, B.D. (2006).
869 Dynamic Regulation of Caveolin-1 Trafficking in the Germ Line and Embryo of
870 *Caenorhabditis elegans*. Mol Biol Cell *17*, 3085 3094.

871 Shivers, R.P., Kooistra, T., Chu, S.W., Pagano, D.J., and Kim, D.H. (2009). Tissue-
872 Specific Activities of an Immune Signaling Module Regulate Physiological Responses to
873 Pathogenic and Nutritional Bacteria in *C. elegans*. Cell Host Microbe *6*, 321–330.

874 Singh, J., and Aballay, A. (2017). Endoplasmic Reticulum Stress Caused by Lipoprotein
875 Accumulation Suppresses Immunity against Bacterial Pathogens and Contributes to
876 Immunosenescence. Mbio *8*, e00778-17.

877 Smulan, L.J., Ding, W., Freinkman, E., Gujja, S., Edwards, Y.J.K., and Walker, A.K.
878 (2016). Cholesterol-Independent SREBP-1 Maturation Is Linked to ARF1 Inactivation.
879 Cell Reports *16*, 9 18.

880 Son, H.G., Altintas, O., Kim, E.J.E., Kwon, S., and Lee, S.V. (2019). Age-dependent
881 changes and biomarkers of aging in *Caenorhabditis elegans*. Aging Cell *18*, e12853.

882 Spang, A. (2002). ARF1 regulatory factors and COPI vesicle formation. Curr Opin Cell
883 Biol *14*, 423–427.

884 Steinbaugh, M.J., Narasimhan, S.D., Robida-Stubbs, S., Mazzeo, L.E.M., Dreyfuss,
885 J.M., Hourihan, J.M., Raghavan, P., Operaña, T.N., Esmaillie, R., and Blackwell, T.K.
886 (2015). Lipid-mediated regulation of SKN-1/Nrf in response to germ cell absence. Elife
887 *4*, 466.

888 Taguchi, T., and Mukai, K. (2019). Innate immunity signalling and membrane trafficking.
889 Curr Opin Cell Biol *59*, 1–7.

890 Tillman, E.J., Richardson, C.E., Cattie, D.J., Reddy, K.C., Lehrbach, N.J., Droste, R.,
891 Ruvkun, G., and Kim, D.H. (2018). Endoplasmic Reticulum Homeostasis Is Modulated
892 by the Forkhead Transcription Factor FKH-9 During Infection of *Caenorhabditis*
893 *elegans*. Genetics *210*, genetics.301450.2018.

894 Troemel, E.R., Chu, S.W., Reinke, V., Lee, S.S., Ausubel, F.M., and Kim, D.H. (2006).
895 p38 MAPK regulates expression of immune response genes and contributes to
896 longevity in *C. elegans*. Plos Genet *2*, e183.

897 Walker, A.K., Jacobs, R.L., Watts, J.L., Rottiers, V., Jiang, K., Finnegan, D.M., Shioda,
898 T., Hansen, M., Yang, F., Niebergall, L.J., et al. (2011). A Conserved SREBP-
899 1/Phosphatidylcholine Feedback Circuit Regulates Lipogenesis in Metazoans. Cell *147*,
900 840 852.

901 Watts, J.L., and Browse, J. (2002). Genetic dissection of polyunsaturated fatty acid
902 synthesis in *Caenorhabditis elegans*. Proc National Acad Sci *99*, 5854 5859.

bioRxiv preprint doi: https://doi.org/10.1101/2021.11.16.468795; this version posted November 16, 2021. The copyright holder for this preprint (which was not certified by peer review) is the author/funder, who has granted bioRxiv a license to display the preprint in perpetuity. It is made available under aCC-BY-NC 4.0 International license.

903 Wellen, K.E., and Thompson, C.B. (2010). Cellular Metabolic Stress: Considering How
904 Cells Respond to Nutrient Excess. Mol Cell *40*, 323 332.

905 Wu, S., and Näär, A.M. (2019). SREBP1-dependent de novo fatty acid synthesis gene
906 expression is elevated in malignant melanoma and represents a cellular survival trait.
907 Sci Rep-Uk *9*, 10369.

908 Wu, Z., Isik, M., Moroz, N., Steinbaugh, M.J., Zhang, P., and Blackwell, T.K. (2019).
909 Dietary Restriction Extends Lifespan through Metabolic Regulation of Innate Immunity.
910 Cell Metab *29*, 1192-1205.e8.

911 Yang, F., Vought, B.W., Satterlee, J.S., Walker, A.K., Sun, Z.-Y.J., Watts, J.L.,
912 DeBeaumont, R., Saito, R.M., Hyberts, S.G., Yang, S., et al. (2006). An ARC/Mediator
913 subunit required for SREBP control of cholesterol and lipid homeostasis. Nature *442*,
914 700 704.

915 Yarwood, R., Hellicar, J., Woodman, P.G., and Lowe, M. (2020). Membrane trafficking
916 in health and disease. Dis Model Mech *13*, dmm043448.

917 Yukselen, O., Turkyilmaz, O., Ozturk, A.R., Garber, M., and Kucukural, A. (2020).
918 DolphinNext: a distributed data processing platform for high throughput genomics. Bmc
919 Genomics *21*, 310.

920 Zmora, N., Bashiardes, S., Levy, M., and Elinav, E. (2017). The Role of the Immune
921 System in Metabolic Health and Disease. Cell Metab *25*, 506–521.

922

bioRxiv preprint doi: https://doi.org/10.1101/2021.11.16.468795; this version posted November 16, 2021. The copyright holder for this preprint (which was not certified by peer review) is the author/funder, who has granted bioRxiv a license to display the preprint in perpetuity. It is made available under aCC-BY-NC 4.0 International license.

A

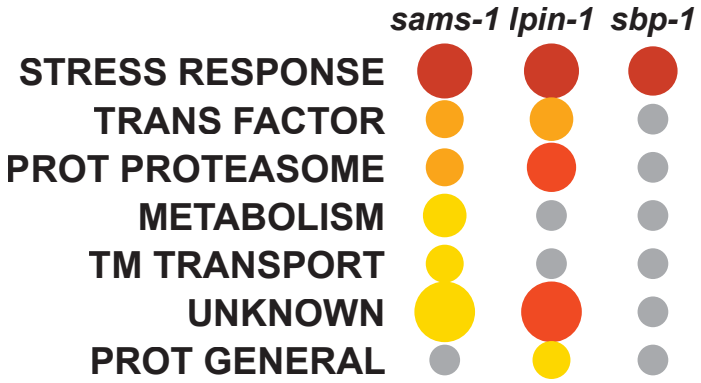

C

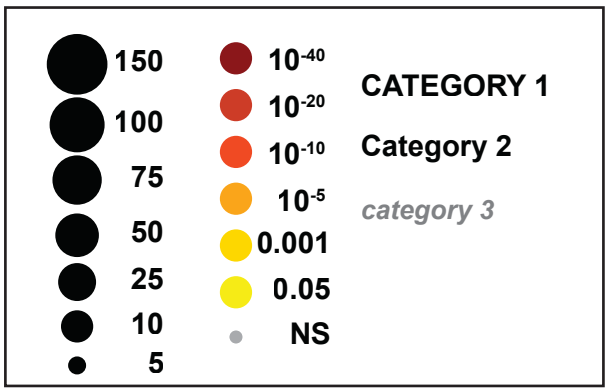

B

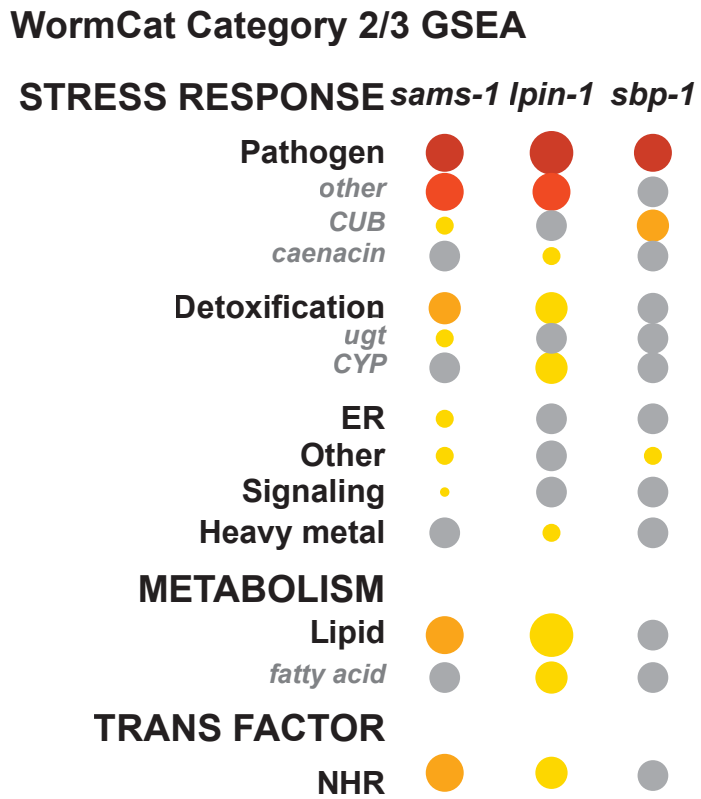

D

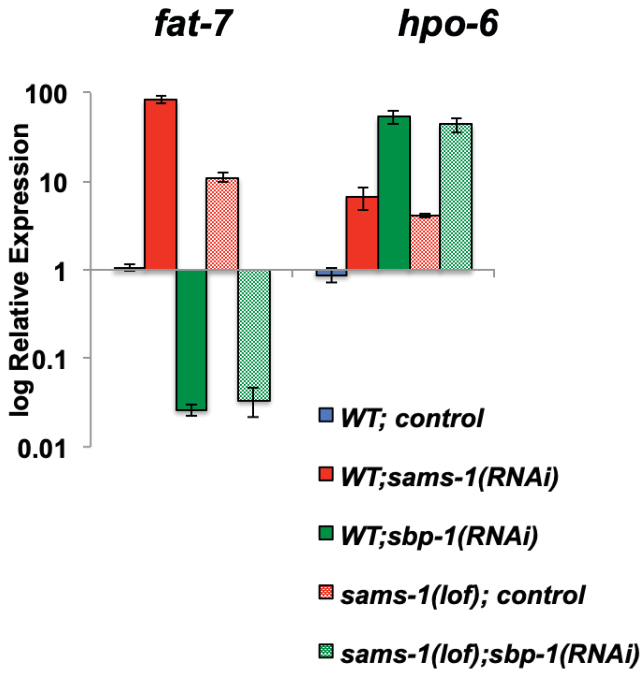

bioRxiv preprint doi: https://doi.org/10.1101/2021.11.16.468795; this version posted November 16, 2021. The copyright holder for this preprint (which was not certified by peer review) is the author/funder, who has granted bioRxiv a license to display the preprint in perpetuity. It is made available under aCC-BY-NC 4.0 International license.

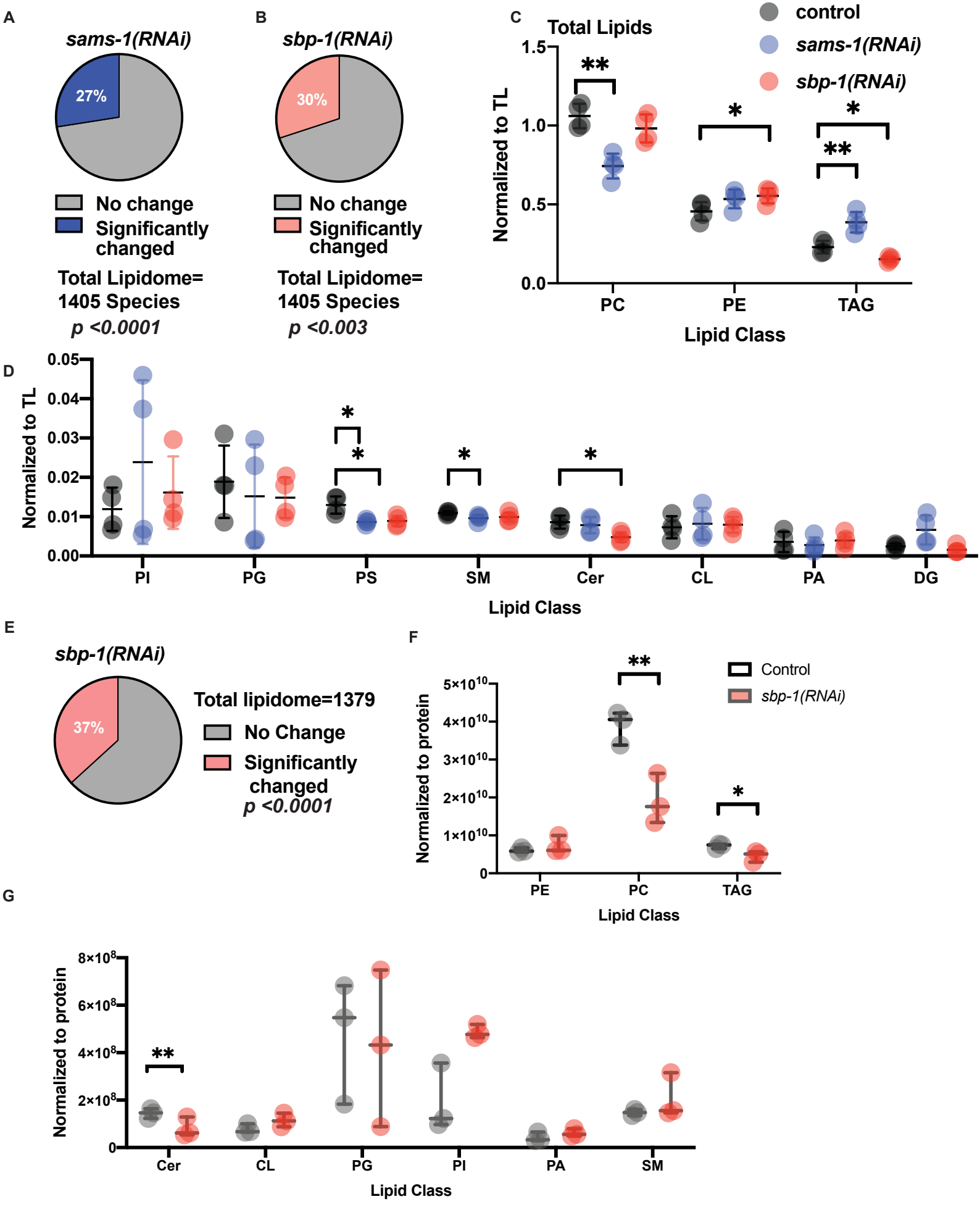

bioRxiv preprint doi: https://doi.org/10.1101/2021.11.16.468795; this version posted November 16, 2021. The copyright holder for this preprint (which was not certified by peer review) is the author/funder, who has granted bioRxiv a license to display the preprint in perpetuity. It is made available under aCC-BY-NC 4.0 International license.

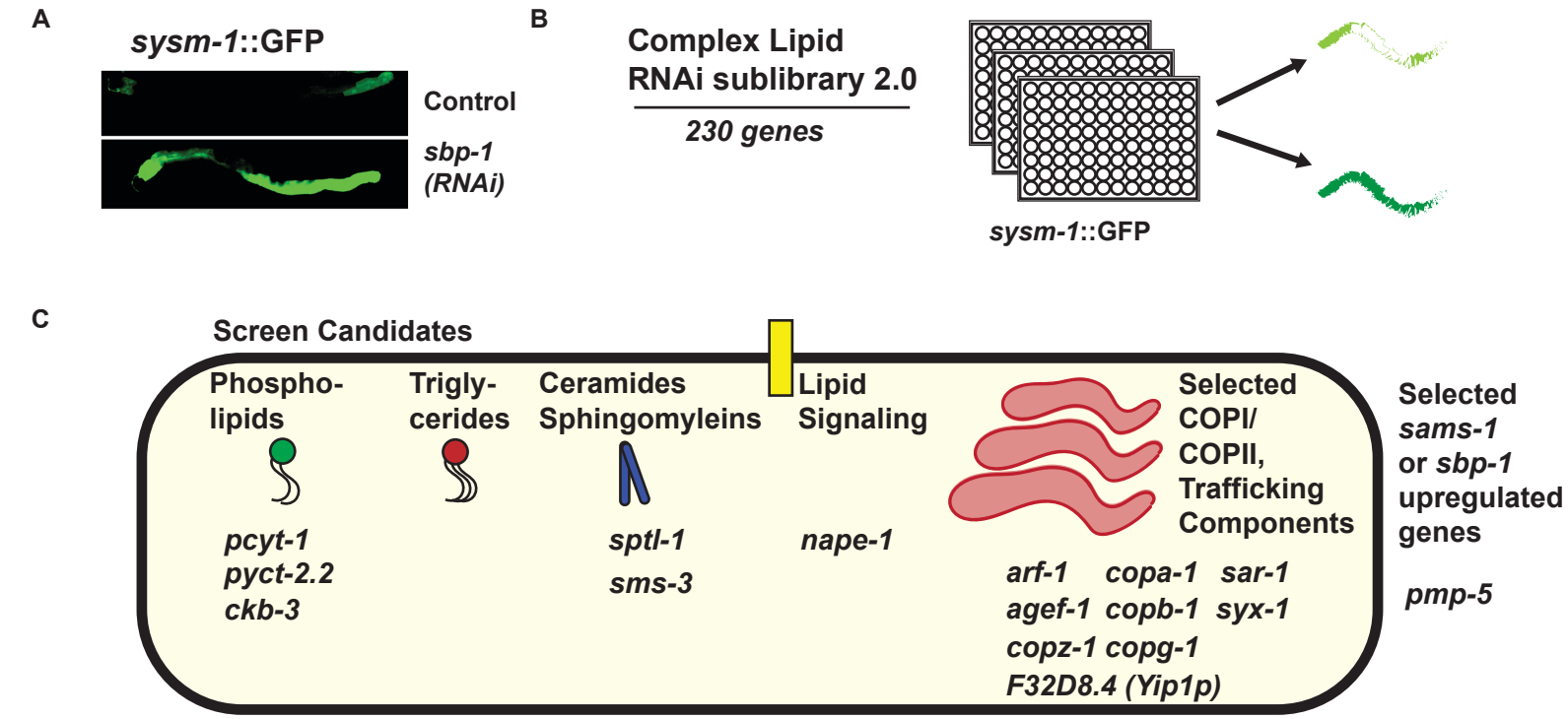

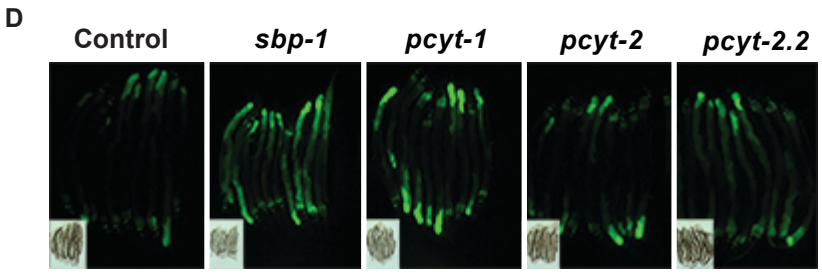

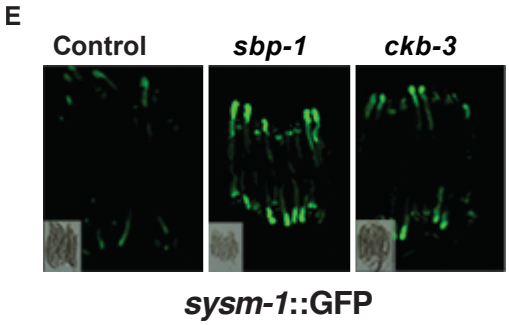

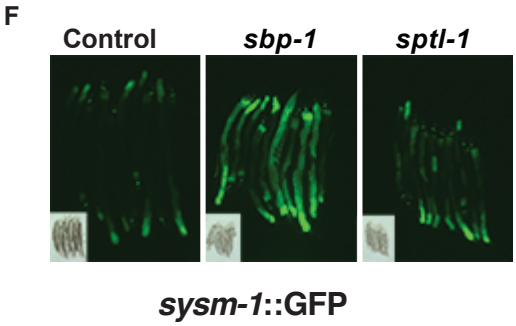

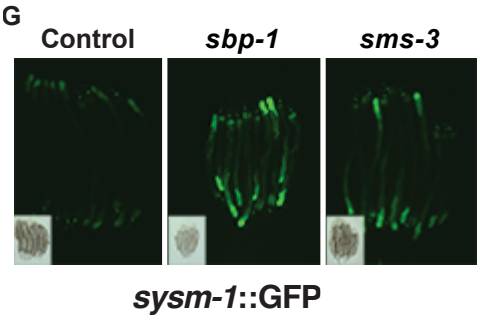

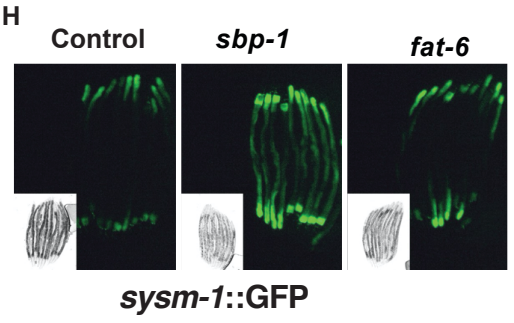

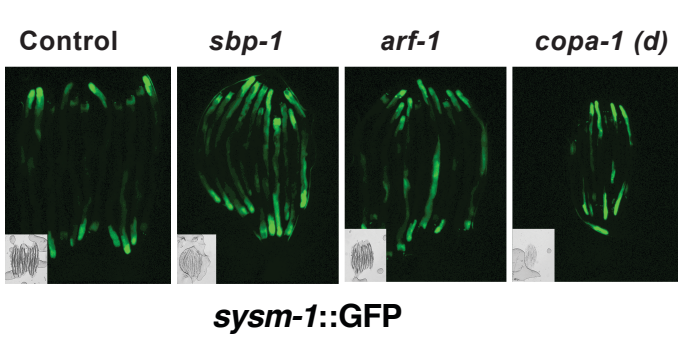

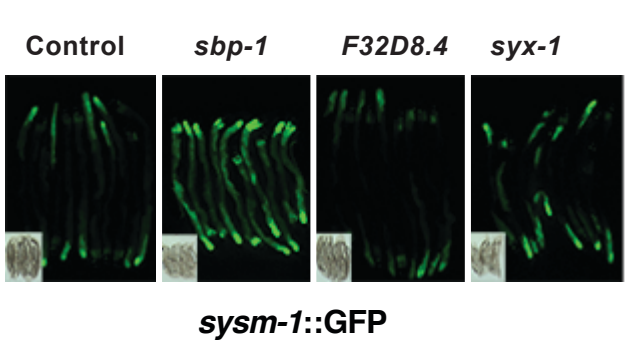

bioRxiv preprint doi: https://doi.org/10.1101/2021.11.16.468795; this version posted November 16, 2021. The copyright holder for this preprint (which was not certified by peer review) is the author/funder, who has granted bioRxiv a license to display the preprint in perpetuity. It is made available under aCCBY-NC 4.0 International license.

A

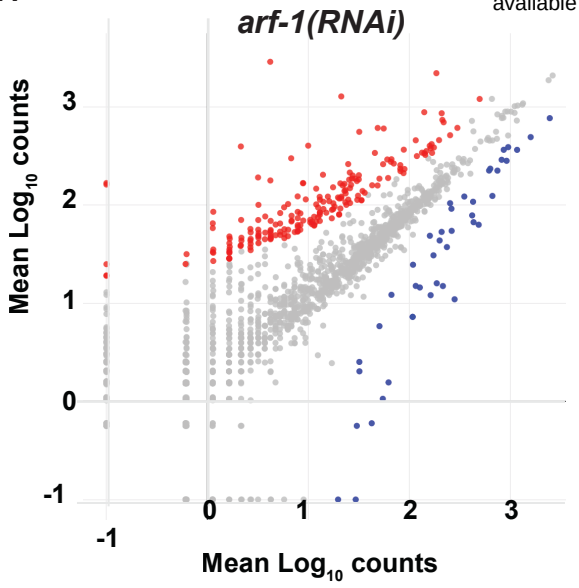

B

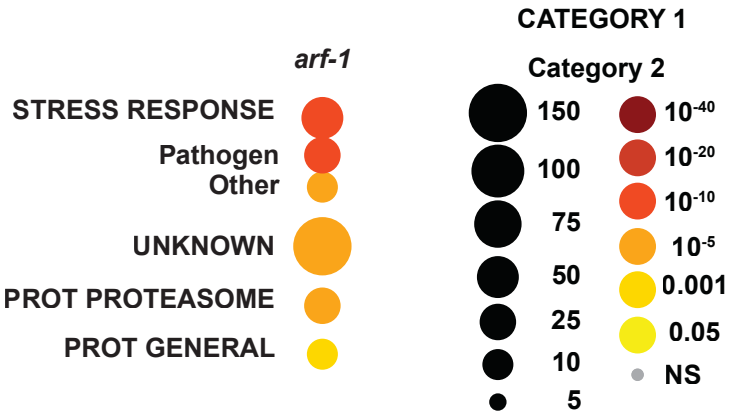

C

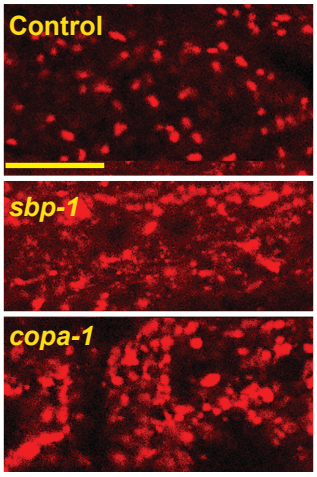

D

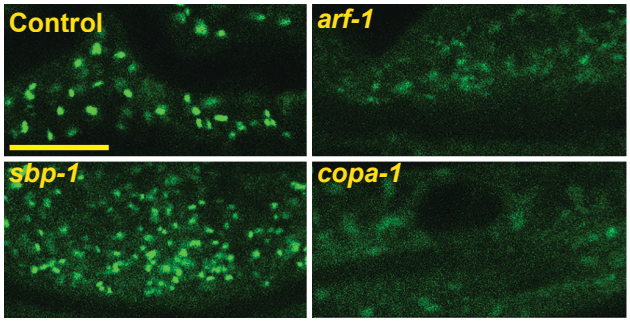
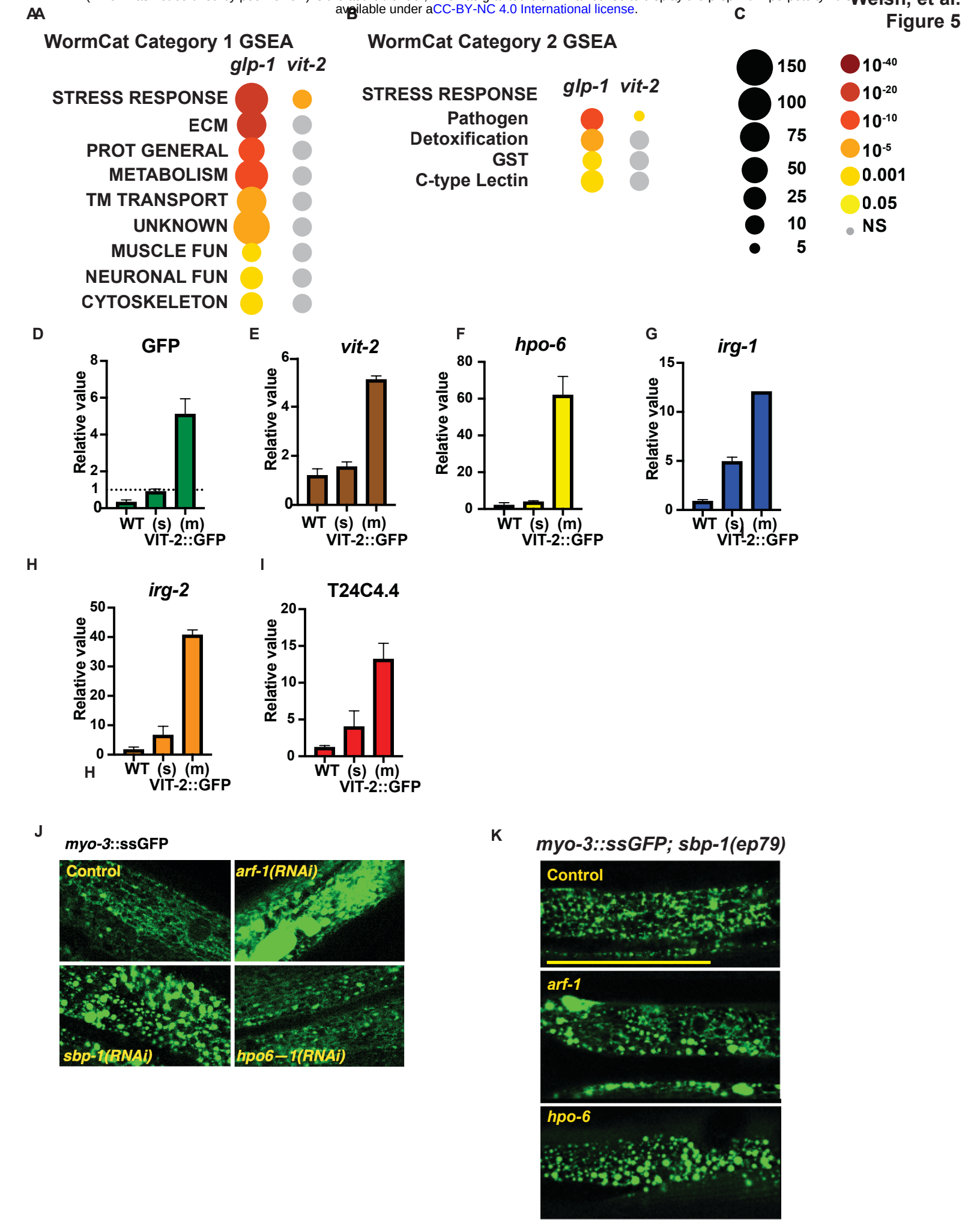
bioRxiv preprint doi: https://doi.org/10.1101/2021.11.16.468795; this version posted November 16, 2021. The copyright holder for this preprint (which was not certified by peer review) is the author/funder, who has granted bioRxiv a license to display the preprint in perpetuity. It is made available under aCC-BY-NC 4.0 International license.